Multivariate AutoRegressive Smooth Liquidity (MARSLiQ)

Christian M. Hafner*[a], Oliver B. Linton†[b], and Linqi Wang‡[c]

[a]Louvain Institute of Data Analysis and Modelling in economics and statistics (LIDAM), and ISBA, UCLouvain
[b]Faculty of Economics, University of Cambridge
[c]School of Mathematical Sciences, Queen Mary University of London

November 24, 2025

Abstract

We propose MARSLiQ (Multivariate AutoRegressive Smooth Liquidity), a new multivariate model for daily liquidity that combines slowly evolving trends with short-run dynamics to capture both persistent and transitory liquidity movements. In our framework, each asset's liquidity is decomposed into a smooth time-varying trend component and a stationary short-run component, allowing us to separate long-term liquidity levels from short-term fluctuations. The trend for each asset is estimated nonparametrically and further decomposed into a common market trend and idiosyncratic (asset-specific) trends, and seasonal trends, facilitating interpretation of market-wide liquidity shifts versus firm-level effects. We introduce a novel dynamic structure in which an asset's short-run liquidity is driven by its own past liquidity as well as by lagged liquidity of a broad liquidity index (constructed from all assets). This parsimonious specification—combining asset-specific autoregressive feedback with index-based spillovers—makes the model tractable even for high-dimensional systems, while capturing rich liquidity spillover effects across assets. Our model's structure enables a clear analysis of permanent vs. transitory liquidity shocks and their propagation throughout the market. Using the model's Vector MA representation, we perform forecast error variance decompositions to quantify how shocks to one asset's liquidity affect others over time, and we interpret these results through network connectedness measures that map out the web of liquidity interdependence across assets.

Keywords: Forecast Error Decomposition; Liquidity Spillovers; Multiplicative Error Model; Network Connectedness; Nonparametric trends

JEL Classification: C12, C14, C32, C53, C58.

*Email: christian.hafner@uclouvain.be.
†Email: obl20@cam.ac.uk.
‡Corresponding author; Email: linqi.wang@qmul.ac.uk; Address: Mile End Road, London, E1 4NS.

1 Introduction

Market liquidity, the ease with which assets can be traded without significantly affecting their price, plays a central role in financial economics. It is well established that liquidity varies over time, both at the individual asset level and across markets, and that such variation can have important implications for asset pricing, risk management, and financial stability. Understanding the dynamics of liquidity and how shocks propagate across assets remains a fundamental challenge, particularly in high-dimensional settings where comovement and spillovers may lead to systemic effects especially during crises, Brunnermeier and Pedersen (2009). While a growing body of literature has explored the commonality in liquidity across assets and its relationship to macroeconomic variables or aggregate market conditions, much of this work relies on parametric or univariate specifications that do not adequately capture the joint dynamics of liquidity across a panel of assets. Existing multivariate models often impose restrictive assumptions or become computationally intractable when applied to large cross-sections of assets. Moreover, standard approaches tend to conflate long-term and short-term movements, obscuring the distinction between persistent trends in liquidity and transitory shocks.

In our earlier work, Hafner et al. (2024), henceforth HLW1, we developed a semiparametric model for daily Amihud-type illiquidity, Amihud (2002), that allowed for a nonparametric trend and short run dynamic components. We used this univariate model to compare trends and dynamics. We extended this work in Hafner et al. (2025), henceforth HLW2, to measure the effects of events such as stock splits on the permanent and temporary components of liquidity. One limitation of these papers is that they were univariate, where nowadays much attention is devoted to understanding the common components of financial variables such as volatility and trading volume. In this paper, we propose a new model Multivariate AutoRegressive Smooth Liquidity (MARSLiQ) that addresses these challenges. Our framework allows for a flexible decomposition of daily liquidity into two interpretable components: a slowly evolving nonparametric trend and a short-run dynamic factor. The trend component captures low-frequency, possibly permanent, shifts in liquidity, with possible seasonal variation, while the dynamic component models high-frequency fluctuations that may be driven by idiosyncratic or common shocks. By modeling the trend

nonparametrically, we avoid imposing arbitrary functional forms and allow for smooth variation over time. We also define a new Generalized Autoregressive Portfolio (GAP) model for the vector short run dynamic components. Specifically, we assume that each asset's short-run liquidity is influenced by its own past values and by the past liquidity of a small number of liquidity indices (constructed as weighted averages across the panel). This structure captures the idea that assets are affected by common liquidity conditions such as those associated with broad funding constraints or aggregate volatility while preserving heterogeneity in asset-level responses. Importantly, this specification facilitates the estimation and interpretation of spillover effects in large systems, making the model scalable and tractable.

To analyze the systemic implications of liquidity shocks, we derive the vector moving average (VMA) representation of the model and develop tools for forecast error variance decomposition and network connectedness analysis. These tools allow us to quantify the contribution of shocks from one asset to the forecast variance of another, thus capturing the directional nature of liquidity spillovers. We consider a number of approaches to identify the structural shocks: the Cholesky decomposition, the Spectral decomposition and the independent component analysis (ICA), exploiting the non-Gaussian features commonly observed in liquidity data.

We apply our methodology to daily liquidity measures of exchange-traded funds (ETFs) from the G7 countries plus Australia and Hong Kong, covering 1996-2025. We first estimate smooth long-run liquidity trends, showing that global liquidity improved before the Global Financial Crisis (GFC), deteriorated sharply during it, and later stabilized with temporary stress episodes around COVID-19 and post-2021 monetary tightening. Country-specific deviations highlight that the U.S. consistently enjoys the deepest liquidity, while Italy remains persistently illiquid. We also investigate potential time-varying seasonal effects in the illiquidity trend and our results indicate that liquidity tends to be lowest around weekends, i.e. on Mondays and Fridays, while it generally improves on Tuesdays. The liquidity level on Wednesdays exhibits pronounced fluctuations over time which could be linked to recurring macroeconomic announcements by major central banks mostly taking place on Wednesdays and Thursdays. Short-run dynamics reveal that domestic liquidity is mainly driven by own past liquidity, but significant spillovers also arise from global liquidity

indices, especially the U.S., which exerts strong negative effects on other markets' short-term liquidity. The variance decomposition and connectedness analysis further demonstrate how shocks propagate across countries, with results emphasizing the systemic role of U.S. liquidity and the time-varying network of liquidity interdependence.

Literature Review. The multiplicative error model (MEM) was introduced in Engle (2002) as a generalization of the ARCH and GARCH models to other financial time series that are non-negative valued. Engle and Rangel (2008) introduced a nonparametric trend to capture the slow moving component of univariate volatility as a multiplicative factor to a standard GARCH model. Hafner and Linton (2010) extended this work to the multivariate GARCH model and derived a full set of inference tools including a discussion about semi-parametric efficiency. Multivariate GARCH models are surveyed in Bauwens et al. (2006). Cipollini et al. (2006) introduced the multivariate MEM and discussed GMM estimation in Cipollini et al. (2013). Barigozzi et al. (2014) introduced a seminonparametric vector MEM process (svMEM) and applied it to realized volatility. Their model had univariate nonparametric trends and univariate (diagonal) dynamics, and they used a copula to model the multivariate i.i.d. error distribution. Cipollini and Gallo (2025) reviewed the progress of MEM models. They also introduce a multivariate multiplicative error model (MEM) and apply it to a trivariate system of realized volatilities. They have only one nonparametric trend component, and they work with i.i.d. shocks. They avoid specifying an error distribution for some well stated reasons and instead use GMM to estimate the dynamic parameters of an unrestricted vector dynamic process. VLAB implements what they call SPLINE-MEM for illiquidity. On the empirical side a number of papers have documented commonality in liquidity measures using less formal methods. Chordia et al. (2000) document that liquidity measures (bid-ask spreads, market depth, etc.) for individual NYSE stocks move together due to market-wide and industry-wide factors even after controlling for firm-specific determinants like volatility, volume, and price. Their methodology was static (time series) regressions for each stock of its daily liquidity measure on market-wide and industry-wide liquidity as well as stock specific controls. Hasbrouck and Seppi (2001) conduct an empirical analysis of the 30 Dow Jones stocks using principal components to investigate common factors in returns, trade order flows, and liquidity. They find that the common factors in traditional liquidity measures (bid-ask spreads, quote sizes, depth)

are relatively small. In other words, while trading activity is synchronized across stocks, liquidity co-movements were modest in their sample, suggesting that idiosyncratic liquidity shocks dominate for large stocks.

2 Multivariate Model

We extend the Cipollini and Gallo (2025) svMEM to allow for different trends by unit and by seasonal component, e.g., day of the week effects. We suppose that for $i = 1, \ldots, N$ we have the multiplicative structure:

$$\ell_{it} = \left(\prod_{j=1}^{J} g_{i,j}(t/T)^{D_{jt}} \right) \lambda_{i,t} \zeta_{i,t} \tag{1}$$

$$\lambda_t = \omega + B\lambda_{t-1} + \Gamma \ell^*_{t-1}, \tag{2}$$

where $g_{i,j}(.)$ are unknown functions of rescaled time, and $\ell^*_{it} = \ell_{it} / \left(\prod_{j=1}^{J} g_{i,j}(t/T)^{D_{jt}} \right)$ is the detrended and deseasonalized liquidity of the i-th unit, while D_{jt} are mutually exclusive and exhaustive dummy variables with $j = 1, \ldots, J$, where $D_{jt} = 1$ if day t is in category j (e.g., day t is Monday), and zero otherwise. Here, ω, λ_t are $N \times 1$ vectors, while B, Γ are $N \times N$ matrices. Let $\mathcal{F}_{it}$ be the information set generated by the i-th asset liquidity up to time t, i.e. $\ell_{i\tau}, \tau \leq t$, and let $\mathcal{F}_t$ be the information set generated by all assets up to time t, i.e. $\ell_{i\tau}, \tau \leq t, i = 1, \ldots, N$. The error process ζ_{it} satisfies $\zeta_{it} \geq 0$ and we suppose that for all i

$$E(\zeta_{it} | \mathcal{F}_{t-1}) = 1,$$

which is the main assumption for estimation. For identification we impose that $E(\lambda_{it}) = 1$ by setting $\omega = (I_N - B - \Gamma)\, i_N$, where i_N is the $N \times 1$ vector of ones. It follows from this that $E(\ell_{it}) = g_{i,j}(t/T)$ if day t is in category j. If the spectral radius of $B + \Gamma$ is less than one, then ℓ^*_t and λ_t are stationary in mean. If the shock distribution is i.i.d., the process λ_t is strictly stationary under conditions on the matrices B and Γ and the distribution of the error, Boussama (1998). The general model is similar to the multivariate svMEM discussed in Cipollini and Gallo (2025), with the already noted distinction that we allow different trends across the units and across the seasonal components.

We can write the model in matrix notation

$$\ell_t = G_t \times \Lambda_t \times \zeta_t,$$

where $\ell_t = (\ell_{1t}, \ldots, \ell_{Nt})^\intercal$, $\zeta_t = (\zeta_{1t}, \ldots, \zeta_{Nt})^\intercal$, $G_t = \prod_{j=1}^{J} \text{diag}(g_{1,j}(t/T)^{D_{jt}}, \ldots, g_{N,j}(t/T)^{D_{jt}})$, and $\Lambda_t = \text{diag}(\lambda_{1t}, \ldots, \lambda_{Nt})$. It follows that

$$E(\ell_t|\mathcal{F}_{t-1}) = G_t \times \Lambda_t \times i_N, \quad E(\ell_t^*|\mathcal{F}_{t-1}) = \Lambda_t \times i_N = \lambda_t, \tag{3}$$

where $\ell_t^* = (\ell_{1t}^*, \ldots, \ell_{Nt}^*)^\intercal$. Suppose that $\text{var}(\zeta_t|\mathcal{F}_{t-1}) = E(\zeta_t\zeta_t^\intercal|\mathcal{F}_{t-1}) - i_N i_N^\intercal = \Omega_t$, then we can obtain that

$$\text{var}(\ell_t|\mathcal{F}_{t-1}) = G_t \times \Lambda_t \times \Omega_t \times \Lambda_t \times G_t, \quad \text{var}(\ell_t^*|\mathcal{F}_{t-1}) = \Lambda_t \times \Omega_t \times \Lambda_t.$$

A common assumption here would be to make ζ_t i.i.d. in which case $\Omega_t = \Omega$ is time invariant. Some authors exploit this further restriction for estimation. Engle and Campos-Martins (2023) argue in a related context that such an assumption is not supported by the data. They develop a model for Ω_t in the large N case. Specifically, $\Omega_t = v_t ss^\intercal$ for a scalar time varying unobserved "factor" v_t and an $N \times 1$ vector of unknown parameters s. We instead suppose that Ω_t is a smooth function of time, i.e., $\Omega_t = \Omega(t/T)$ for some matrix of smooth functions $\Omega(\cdot)$. By allowing for time variation we break the otherwise strong link between $E(\ell_t^*|\mathcal{F}_{t-1})$ and $\text{var}(\ell_t^*|\mathcal{F}_{t-1})$, allowing for overdispersion. This does not affect our estimation strategy for B, Γ, and $g(.)$, but it does affect our variance decompositions as we discuss below. Note that under this weaker assumption, although the process λ_t is mean stationary it is not weakly stationary, since the covariance matrix is time varying. Nevertheless, it can be shown to be locally weakly stationary, Dahlhaus (1997), and one can derive an expression for its unconditional variance, which we give in the Appendix.

2.1 Nonparametric Trends

Cipollini and Gallo (2025) work with a single common nonparametric trend, i.e., they suppose that $g_i(u) = \mu_i g_0(u)$ for some univariate function $g_0(.)$ and unconditional mean μ_i and ignore the seasonal effect. We propose a test for this restriction inside our more general specification that does not restrict $g_{i,j}$. In our application we find this restriction to be

strongly rejected, so we work with the general model, but we also consider a decomposition of the trends into common and idiosyncratic components for interpretation purposes.

We define the common trend as

$$g_0(u) = \sum_{i=1}^{N}\sum_{j=1}^{J} \vartheta_{i,j} g_{i,j}(u), \tag{4}$$

where $\vartheta_{i,j} \geq 0$ are observed weights, with $\sum_{i=1}^{N}\sum_{j=1}^{J} \vartheta_{i,j} = 1$, such as market cap or equal weighting. Then define the firm specific or idiosyncratic trend $g_i^{\&}(u)$ and the time varying global seasonal component $g_j^{\%}(u)$

$$g_i^{\&}(u) = \sum_{j=1}^{J} \psi_j \frac{g_{i,j}(u)}{g_0(u)}, \quad g_j^{\%}(u) = \sum_{i=1}^{N} \tau_i \frac{g_{i,j}(u)}{g_0(u)},$$

where ψ_j, τ_i are weights. These are well defined for any functions $g_{i,j}$. We may further define the average seasonal effect as $s_j = \int_0^1 g_j^{\%}(u)du$. We may interpret these components within a multiplicative model of the form

$$g_{i,j}(u) = g_0(u) g_i^{\&}(u) g_j^{\%}(u), \tag{5}$$

subject to the identifying restrictions. For example, if we take all weights to be equal, and we suppose that $\sum_{i=1}^{N} g_i^{\&}(u) = 1$ and $\sum_{j=1}^{J} g_j^{\%}(u) = 1$, then the components line up. If we specify a parametric model for the seasonal component such as $g_j^{\%}(u) = s_j$ for all u, then the integrated component function satisfies $\int_0^1 g_j^{\%}(u)du = s_j$.

2.2 Generalized Autoregressive Portfolio Model

In large dimensional cases, estimating the matrices of parameters $B = (\beta_{ij})_{i,j=1}^{N}$, $\Gamma = (\gamma_{ij})_{i,j=1}^{N}$ is difficult computationally, and the large number of parameters poses issues for inference and interpretability. There are a number of approaches to restricting the parameter space dimensionality. For example, one can assume that B, Γ are lower (or upper) triangular matrices, based on some ordering of the units. The diagonal assumption that $B = \text{diag}\{\beta_1, \ldots, \beta_N\}$ and $\Gamma = \text{diag}\{\gamma_1, \ldots, \gamma_N\}$ is commonly used, see Barigozzi et al. (2014), but is an even stronger restriction on the dynamics. Another approach is to impose a sparsity assumption on the off-diagonal elements of B, Γ. Here, we suggest a slightly more general restriction that reduces the dimensionality of the parameter space to order N.

Definition 1. *The Generalized Autoregressive Portfolio model, GAP(1,1,R). We suppose that the matrices* B, Γ *satisfy*

$$B = D_B + B^* W^\intercal, \quad \Gamma = D_\Gamma + D^* W^\intercal, \tag{6}$$

where $B^* = (b^*_{ir})$ *and* $D^* = (\delta^*_{ir})$ *are* $N \times R$ *matrices of free parameters and* D_B, D_Γ *are diagonal matrices with elements* β_{ii}, γ_{ii} *respectively. Here,* W *is an* $N \times R$ *matrix of known portfolio weights that satisfy* $W^\intercal i_N = i_R$*, these could be equal weighting or market cap weighting or price weighting or whatever.*

This structure seems natural in financial applications where portfolios are often interpreted as providing meaningful systematic factors. Recent work in the networks literature (see for example Knight et al. (2016) and Nason et al. (2025)) has proposed a similar structure where the matrix W is picking out network neighbors and weighting them.[1] A key feature of this model is that it imposes linear restrictions on the parameter matrices B, Γ, which is convenient for testing purposes. Let Ψ_N be the $N \times N^2$ matrix of zeros and ones defined in Magnus (1988, p109) that satisfies $\Psi_N^\intercal d = \text{vec}(D)$ for a diagonal matrix D with diagonal vector d. Then

$$\text{vec}(B) = \Psi_N^\intercal d_B + (W \otimes I_N)\,\text{vec}(B^*), \quad \text{vec}(\Gamma) = \Psi_N^\intercal d_\Gamma + (W \otimes I_N)\,\text{vec}(D^*),$$

where d_B, d_Γ are the $N \times 1$ vectors with typical elements β_{ii} and γ_{ii} respectively. That is, $\text{vec}(B) = \mathcal{L}_B \theta$ and $\text{vec}(\Gamma) = \mathcal{L}_\Gamma \theta$ for known matrices $\mathcal{L}_B, \mathcal{L}_\Gamma$, where θ contains the free parameters in d_B, d_Γ, $\text{vec}(B^*)$, and $\text{vec}(D^*)$. Furthermore, we can write for each unit i

$$\lambda_{it} = \omega_i + \beta_{ii}\lambda_{i,t-1} + \sum_{r=1}^{R} b^*_{ir}\lambda_{w_r,t-1} + \gamma_{ii}\ell^*_{i,t-1} + \sum_{r=1}^{R} \delta^*_{ir}\ell^*_{w_r,t-1} \tag{7}$$

where $\omega_i = 1 - \beta_{ii} - \sum_{r=1}^{R} b^*_{ir} - \gamma_{ii} - \sum_{r=1}^{R} \delta^*_{ir}$ for identification. The series $\ell^*_{w_r,t} = \sum_{i=1}^{N} w_{ir}\ell^*_{i,t}$ are observable and each represents an index of liquidity (rather than the liquidity of the index), whereas $\lambda_{w,t} = E(\ell^*_{w,t}\,|\mathcal{F}_{t-1}) = W^\intercal \lambda_t \in \mathbb{R}^r$ is defined as

$$\lambda_{w,t} = \omega^\dagger + W^\intercal D_B \lambda_{t-1} + B^\dagger \lambda_{w,t-1} + W^\intercal D_\Gamma \ell^*_{t-1} + D^\dagger \ell^*_{w,t-1},$$

[1] In that literature it is conventional to set the diagonal elements of W to zero. Nason et al. (2025) establish a number of theoretical properties of this class of processes including stationarity.

where $\omega^\dagger = W^\intercal \omega$, $B^\dagger = W^\intercal B^*$, and $D^\dagger = W^\intercal D^*$. The series $\lambda_{w,t}$ is unobservable and in general depends on all the latent values $\lambda_{i,t}$ and hence all the parameters of the system; therefore, estimation still needs to be done at a system level. There are $2N(R+1)$ unknown parameters, which represents a big reduction in dimensionality but if N is large, system estimation may be challenging.

There are several special cases of this model where estimation can be simplified.

Definition 2. *Model GAPD. Suppose that (6) holds and that $B^* = 0$ so that*

$$B = D_B, \quad \Gamma = D_\Gamma + D^* W^\intercal,$$

so that B is a diagonal matrix.

In this case the equation for $\lambda_{w,t}$ simplifies to $\lambda_{w,t} = \omega^\dagger + B^\dagger \lambda_{w,t-1} + W^\intercal D_\Gamma \ell^*_{t-1} + D^\dagger \ell^*_{w,t-1}$. Furthermore, the equation for λ_{it} depends only on past observables and its own lag and its own parameters. Specifically,

$$\lambda_{it} = \omega_i + \beta_{ii}\lambda_{i,t-1} + \gamma_{ii}\ell^*_{i,t-1} + \delta_i^{*\intercal} \ell^*_{w,t-1}, \tag{8}$$

where $\omega_i = 1 - \beta_{ii} - \gamma_{ii} - \sum_{r=1}^R \delta^*_{ir}$. This dynamic equation only depends on the observables $\ell^*_{i,t-1}, \ell^*_{w,t-1}, \ldots$. and on the parameters $\omega_i, \beta_{ii}, \gamma_{ii}, \delta^*_i$. This allows spillovers from other firms' liquidity only through the index effect, but it allows for heterogeneity in all parameters. In this case there are $N(2+R)$ parameters in total. This special case can be estimated by single equation methods, since it only depends on the parameters indexed by i. Specifically, one can estimate the $R+2$ free parameters for each asset using data only on that asset.

Definition 3. *Model GAPC. Suppose that (6) holds and that there exist $R \times R$ matrices A, C for which*

$$W^\intercal D_B = A W^\intercal, \quad W^\intercal D_\Gamma = C W^\intercal. \tag{9}$$

In this case we can write the equation for aggregate dynamic liquidity as

$$\lambda_{w,t} = W^\intercal \lambda_t = \omega^\dagger + A^\dagger \lambda_{w,t-1} + D^\dagger \ell^*_{w,t-1}, \tag{10}$$

where $\omega^\dagger = W^\intercal \omega$, $A^\dagger = A + W^\intercal B^*$, and $D^\dagger = C + W^\intercal D^*$. The key thing is that the equation for $\lambda_{w,t}$ can in this case be expressed purely in terms of the $R \times 1$ vectors $\lambda_{w,t-1}, \ell^*_{w,t-1}$. We

can therefore express $\lambda_{w,t}$ in terms of the observables $\ell^*_{w,t-1}, \ell^*_{w,t-2}, \ldots$ and substitute $\lambda_{w,t-1}$ out of the individual asset equation (7). For example, suppose that $\beta_{ii} = \beta$ and $\gamma_{ii} = \gamma$, which is consistent with (9). Then, we have

$$\lambda_{it} = \omega_i + \beta\lambda_{i,t-1} + b_i^{*\intercal}\lambda_{w,t-1} + \gamma\ell^*_{i,t-1} + \delta_i^{*\intercal}\ell^*_{w,t-1}, \tag{11}$$

where $\lambda_{w,t} = \omega^\dagger + A^\dagger\lambda_{w,t-1} + D^\dagger\ell^*_{w,t-1}$. This model allows for more complicated spillovers from the index but at the cost of restricting the own effects to be homogeneous. In this case, λ_{it} only depends on the observables $\ell^*_{i,t-1}, \ell^*_{w,t-1}, \ldots,$, where $\ell^*_{w,t-1} \in \mathbb{R}^R$ are low dimensional. This structure is convenient in estimation, see below.

3 Forecasting

In this section we discuss forecasting in the multivariate setting. Our models allow for spillovers of liquidity shocks to one asset to affect liquidity of another asset and we show how to capture this in our framework. For simplicity we ignore seasonality and suppose that $g_{i,j} = g_i$ for all i, j. We sketch out the arguments here based on knowledge of the unknown quantities; in practice we replace them by estimates defined in the next section. We will use the notation from the general model for simplicity. We first note that the optimal one-step ahead forecast for detrended liquidity ℓ^*_{t+1} given all information at time t is

$$\ell^*_{t+1|t} = E\left(\ell^*_{t+1}\,|\mathcal{F}_t\right) = \lambda_{t+1} = \omega + B\lambda_t + \Gamma\ell^*_t \tag{12}$$

The prediction error of this forecast is

$$\xi_{t+1} = \Lambda_{t+1}(\zeta_{t+1} - i_N) = (\xi_{1,t+1}, \ldots, \xi_{N,t+1})^\intercal.$$

This is a vector MDS with conditional variance $\Lambda_{t+1}\Omega((t+1)/T)\Lambda_{t+1}$, and unconditional variance

$$\Sigma((t+1)/T) = E\left(\Lambda_{t+1}\Omega((t+1)/T)\Lambda_{t+1}\right), \tag{13}$$

which we calculate below. Following Fan and Gijbels (1996) we may forecast the future nonparametric trend $g((t+1)/T)$ by the current value $g(t/T)$, justified by the one term Taylor series approximation. One may employ the refined forecast $g(t/T) + g'(t/T)/T$, but

neither in theory nor in practice is this worth the effort, because the estimation error in $g(t/T)$ will be of larger order than $1/T$. Therefore, we forecast the future liquidity itself ℓ_{t+1} by

$$\ell_{t+1|t} = E\left(\ell_{t+1}\,|\mathcal{F}_t\right) \simeq G(t/T)\Lambda_{t+1}i_N,$$

where $G(t/T), \Lambda_{t+1}$ are the diagonal matrices containing $g_i(t/T)$ and $\lambda_{i,t+1}$ respectively. The forecast error covariance matrix for ℓ_{t+1} is approximately $G(t/T)\Sigma(t/T)G(t/T)$.

The multistep forecast for ℓ^*_{t+h} is

$$\ell^*_{t+h|t} = \omega + (B+\Gamma)\,\lambda_{t+h-1|t} \tag{14}$$

To analyze the multistep forecast error we work with the VMA(∞) representation for ℓ^*_t.

$$\ell^*_t = i_N + \sum_{j=0}^{\infty} \Phi_j \xi_{t-j}, \tag{15}$$

where $\Phi_0 = I_N$, $\Phi_1 = \Gamma$ and $\Phi_i = (B+\Gamma)\Phi_{i-1}$, $i \geq 2$, see e.g. Lütkepohl (2005). Consequently, the forecast error has conditional mean zero and unconditional variance $\sum_{j=0}^{h-1} \Phi_j \Sigma((t+j)/T)\Phi_j^\intercal$.

Note that the error terms ξ_t are typically non-orthogonal. In the next subsection we discuss different approaches to how to orthogonalize the shocks.

3.1 Forecast Error Variance Decomposition

Impulse response analysis and forecast error variance decomposition, as popularized by Sims (1980), hinge on an appropriate orthogonalization of the error terms ε_t in (15), for which several methods exist, see e.g. Lütkepohl (2005) for an overview. The original Cholesky-factor identification proposed by Sims (1980) is often used, but is sensitive to the ordering of the variables in the system. The generalized variance decomposition of Pesaran and Shin (1998), which is used in Diebold and Yılmaz (2014), requires normality of the error terms which in our case is not satisfied as these errors will typically be highly skewed.

Suppose $\Sigma(u) = P(u)P(u)^\intercal$, the proportion of the one-step ahead forecast error variance of liquidity i accounted for by innovations in liquidity j is then given by

$$\omega_{ij}(u) = \frac{\left(e_i^\intercal P(u) e_j\right)^2}{e_i^\intercal P(u)P(u)^\intercal e_i}.$$

We consider two decompositions to obtain $P(u)$: i) Cholesky factorization where $P(u)$ is a lower triangular matrix; ii) spectral decomposition with $\Sigma(u) = V(u)M(u)V(u)^\intercal$, where $\Lambda(u)$ is a diagonal matrix and $Q(u)$ is orthonormal. In this case, $P(u) = V(u)M(u)^{1/2}V(u)^\intercal$.

For ℓ_{t+1} the variance decomposition is exactly the same, since the mean trend cancels out ($e_j^\intercal G(u) = g_j$ and this term cancels out top and bottom). Nevertheless, the variance decomposition is time varying due to time variation in $P(u)$. In the multistep prediction the forecast error variance is

$$\omega_{ij,h}(u) = \frac{\sum_{k=0}^{h-1} \left(e_i^\intercal \Phi_k P(u) e_j\right)^2}{\sum_{k=0}^{h-1} e_i^\intercal \Phi_k P(u) P(u)^\intercal \Phi_k^\intercal e_i}, \tag{16}$$

where Φ_k are the coefficient matrices in the MA representation.

An alternative way of finding the underlying structural shocks is based on the independent component analysis (ICA) method which aims to find linear combinations of the error term ε_t that are independent. Justifications for this data-driven identification method have been given by Herwartz and Plödt (2016) in the context of vector autoregressive models, and Hafner et al. (2022) for multivariate GARCH models, among others. It is well known that independent components are identified under non-Gaussian distributions, a feature that is particularly relevant in our case where the error terms are typically highly skewed and far from Gaussian. We therefore expect ICA to deliver well identified and efficiently estimated independent components. We suppose that $u_t^* = \Omega^{-\frac{1}{2}}(t/T)(\zeta_t - i_N)$, which satisfies $E(u_t^*) = 0$ and $E(u_t^* u_t^{*\intercal}) = I_N$. The task of ICA is to find linear combinations of the components of u_t^*,

$$u_t = A u_t^*, \tag{17}$$

with $(N \times N)$ "unmixing" matrix A, such that u_{it} is independent from u_{jt}, $i \neq j$. For identification, A is restricted to be orthogonal so that $\mathrm{Var}(u_t) = I_N$. To obtain the forecast error variance decompositions, we use the VMA(∞) representation (15). Based on the ICA, we can rewrite the model for ℓ_t^* as $\ell_t^* = i_N + \sum_{k=0}^{\infty} \Theta_k(t/T) u_{t-k}$, where $\Theta_k(t/T) := \Phi_k \Lambda_{t-k} \Omega^{1/2}((t-k)/T) A^\intercal$, and u_t are random vectors with zero mean and identity covariance matrix with independent components. In general, $\Theta_k(.) = (\theta_{ij,k}(.))_{i,j=1}^N$ is varying over time driven by the time variation in $\Omega(.)$. The proportion of the h-step ahead forecast error

variance of liquidity i accounted for by innovations in liquidity j is then given by

$$\omega_{ij,h}(u) = \frac{\sum_{k=0}^{h-1}(\theta_{ij,k}(u))^2}{\sum_{j=1}^{N}\sum_{k=0}^{h-1}(\theta_{ij,k}(u))^2}. \tag{18}$$

Note that $\sum_{j=1}^{N}\omega_{ij,h}(u) = 1$. A large proportion $\omega_{ij,h}(u)$ would then indicate that liquidity i's forecast uncertainty, at a given time horizon and given time, is to a large part explained by another liquidity j, and can be interpreted as a spillover effect from liquidity j to liquidity i.

3.2 Network Connectedness

The analysis can be refined following Diebold and Yılmaz (2014) by viewing variance decompositions as weighted directed networks. Denote by $W_h(u) = (\omega_{ij,h}(u)$ the matrix containing all individual elements $\omega_{ij,h}(u)$. Each element of $W_h(.)$ measures the pairwise directional connectedness from j to i at rescaled time u, $C^H_{i\leftarrow j} := \omega_{ij,h}(u)$. Since our variance decomposition matrix is not symmetric , $C^H_{i\leftarrow j} \neq C^H_{j\leftarrow i}$ in general. Therefore, we have $N^2 - N$ different pairwise directional connectedness measures.

The "to" measure is defined as the total direction connectedness to others from j, which measures the sum of the contributions of liquidity j to all other liquidity's forecast errors, and it can be viewed as a "to"-degree of a node (i.e. a liquidity) of the network:

$$C^h_{\cdot\leftarrow j}(u) := \omega_{\cdot j}(u) = \sum_{i=1, i\neq j}^{N}\omega_{ij,h}(u) \tag{19}$$

Likewise, the "from" directional connectedness is defined as the total direction connectedness from others to i, which measures the sum of the contributions of all other liquidities j to explain the forecast error variance of liquidity i:

$$C^h_{i\leftarrow\cdot}(u) := \omega_{i\cdot}(u) = \sum_{j=1, j\neq i}^{N}\omega_{ij,h}(u) \tag{20}$$

Therefore, we have $2N$ total direction connectedness measures, N of which explain the transmitted shocks to others, and the remaining N explain the received shocks from others. Consequently, the net total direction connectedness is equal to $C^H_i = C^H_{\cdot\leftarrow i} - C^H_{i\leftarrow\cdot}$. In total there are $N(N-1)/2$ net pairwise directional connectedness measures, and N net total directional connectedness measures.

Finally, the total connectedness measure for the network of liquidities is the grand total of the off-diagonal elements in the variance decomposition matrix, which is given by

$$C^H : \omega = \sum_{i=1}^{N} \omega_{i\cdot} = \sum_{j=1}^{N} \omega_{\cdot j}. \tag{21}$$

This total connectedness mean degree of the network. The larger the mean degree, the greater the overall network connectedness. In our framework this varies over time in a smooth way. In the empirical part, we will use this methodology to analyse the network connectedness of detrended liquidities, identify important spillover transmitters, and estimate the total connectedness of the system.

4 Estimation

We observe a sample of daily illiquidities $\{\ell_{it},\ t = 1, \ldots, T,\ i = 1, \ldots, N\}$, where $\ell_{it} = HL_{it}/V_{it}$, and HL_{it} is the high-low intraday volatility measure, while V_{it} is the dollar trading volume. We use the high-low volatility for the reasons discussed in HLW2. We next outline the various parts of our estimation procedures.

4.1 Nonparametric Trend

We estimate the trends by the local linear estimator $\widehat{g}_{i,j}(u) = \widehat{\alpha}_{ij}(u)$, where for $u \in [0, 1]$ and $i = 1, \ldots, N$, and $j = 1, \ldots, J$,

$$(\widehat{\alpha}_{ij}(u), \widehat{\beta}_{ij}(u)) = \arg\min_{\alpha,\beta} \sum_{t=1}^{T} K_h(t/T - u) D_{jt} \left\{ \ell_{it} - \alpha - \beta(t/T - u) \right\}^2. \tag{22}$$

Here, $K_h(.) = K(./h)/h$ is a kernel and h is a bandwidth. The local linear estimator is preferred to the local constant because of its superior boundary properties (estimation for small t or large t), Fan and Gijbels (1996).

Define the estimated common trend

$$\widehat{g}_0(u) = \sum_{i=1}^{N} \sum_{j=1}^{J} \vartheta_{i,j} \widehat{g}_{i,j}(u) \tag{23}$$

and the idiosyncratic trend and the time varying global seasonal component:

$$\widehat{g}_i^{\&}(u) = \sum_{j=1}^{J} \psi_j \frac{\widehat{g}_{i,j}(u)}{\widehat{g}_0(u)}, \quad \widehat{g}_j^{\%}(u) = \sum_{i=1}^{N} \tau_i \frac{\widehat{g}_{i,j}(u)}{\widehat{g}_0(u)}.$$

To estimate a seasonal constant s_j, we may take $\widehat{s}_j = \int_0^1 \widehat{g}_j^{\%}(u)du$.

Define the detrended liquidity $\widehat{\ell}_t^* = (\widehat{\ell}_{1t}^*, \ldots, \widehat{\ell}_{Nt}^*)^\intercal$, wher e $\widehat{\ell}_t^* = \widehat{G}_t^{-1}\ell_t$ and (for $t = 1, \ldots, T$), $\widehat{G}_t = \text{diag}(\prod_{j=1}^J \widehat{g}_{1,j}(t/T)^{D_{jt}}, \ldots, \prod_{j=1}^J \widehat{g}_{N,j}(t/T)^{D_{jt}})$. There are several ways to improve these estimates depending on the assumptions that are made about the error as discussed in HLW1. We maintain the weak martingale difference assumption. Define the prewhitened illiquidity $\ell_{it}^\dagger = \ell_{it}/\lambda_{it}$, and note that $E\left(\ell_{it}^\dagger\right) = \prod_{j=1}^J g_{i,j}(t/T)^{D_{jt}}$ also. Let $\widehat{\theta}$ be consistent estimates of θ, see below, and let $\widehat{\ell}_t^\dagger = (\widehat{\ell}_{1t}^\dagger, \ldots, \widehat{\ell}_{Nt}^\dagger)^\intercal$, where $\widehat{\ell}_t^\dagger = \Lambda_t(\widehat{\theta}, \widehat{g})^{-1}\ell_t$. Here, $\Lambda_t(\widehat{\theta}, \widehat{g}) = \text{diag}(\lambda_t(\widehat{\theta}, \widehat{g}))$, where $\lambda_t(\widehat{\theta}, \widehat{g}) = (\lambda_{1t}(\widehat{\theta}, \widehat{g}), \ldots, \lambda_{Nt}(\widehat{\theta}, \widehat{g}))^\intercal$ is defined recursively, i.e., $\lambda_t(\widehat{\theta}, \widehat{g}) = (I_N - \widehat{B} - \widehat{\Gamma})i_N + \widehat{B}\lambda_{t-1}(\widehat{\theta}, \widehat{g}) + \widehat{\Gamma}\widehat{\ell}_{t-1}^*$ with some initial condition. Then for $u \in [0,1]$, let $\widetilde{g}_{i,j}(u) = \widetilde{\alpha}_{ij}(u)$, where $\widetilde{\alpha}_{ij}(u), \widetilde{\beta}_{ij}(u)$ minimize (22) with ℓ_{it} replaced by $\widehat{\ell}_{it}^\dagger$. Let $\widetilde{g}_0(u) = \sum_{i=1}^N \sum_{j=1}^J \vartheta_{i,j}\widetilde{g}_{i,j}(u)$, $\widetilde{g}_i^{\&}(u) = \sum_{j=1}^J \psi_j(\widetilde{g}_{i,j}(u)/\widetilde{g}_0(u))$, and $\widetilde{g}_j^{\%}(u) = \sum_{i=1}^N \tau_i(\widetilde{g}_{i,j}(u)/\widetilde{g}_0(u))$.

4.2 Estimation of Dynamic Parameters by GMM

4.2.1 Full System Approach

We use GMM to estimate the parameters from the conditional moment restriction $E(\zeta_t|\mathcal{F}_{t-1}) = i_N$, $t = 1, \ldots, T$. In the general case let $\theta = (\text{vec}(B)^\intercal, \text{vec}(\Gamma)^\intercal)^\intercal$ (in special cases, θ is the vector of free parameters see above). We work with the vector residual $\zeta_t(\theta, g) - i_N = \Lambda_t(\theta, g)^{-1}\ell_t^* - i_N$, which is a martingale difference sequence at the true parameter values $B = B_0, \Gamma = \Gamma_0$. In practice, we define $\zeta_t(\theta, \widehat{g}) - i_N = \widehat{\Lambda}_t(\theta, g)^{-1}\widehat{\ell}_t^* - i_N$, where $\Lambda_t(\theta, \widehat{g}) = \text{diag}(\lambda_t(\theta, \widehat{g}))$ and $\widehat{\lambda}_t(\theta, \widehat{g}) = (I_N - B - \Gamma)\, i_N + B\lambda_{t-1} + \Gamma\widehat{\ell}_{t-1}^*$ is defined dynamically with some initialization. Then define $\rho_t(\theta, \widehat{g}) = z_{t-1} \otimes (\zeta_t(\theta, \widehat{g}) - i_N)$, where $z_{t-1} \in \mathcal{F}_{t-1}$ are valid instruments, and let

$$\widehat{\theta} = \arg\min_{\theta \in \Theta} \left\| M_T(\theta, \widehat{g}) \right\|_S^2, \quad M_T(\theta, \widehat{g}) = \frac{1}{T}\sum_{t=1}^T \rho_t(\theta, \widehat{g}), \tag{24}$$

where S is a weighting matrix and $\|a\|_S = a^\intercal S a$, while Θ is a parameter space. We typically take lagged values of the residuals as instruments and provided we take enough of these the method is overidentified. We take $S = I_q$, where $\rho_t(\theta, g) \in \mathbb{R}^q$. Since we emphasize robustness over efficiency, this seems appropriate. Based on the preliminary estimator $\widehat{\theta}$

we update our trend estimator to $\widetilde{g}$, and define

$$\widetilde{\theta} = \arg\min_{\theta\in\Theta} \left\| M_T(\theta, \widetilde{g}) \right\|_S^2 . \tag{25}$$

We may iterate further between updating the trend and updating the dynamic parameters but theoretically two rounds is sufficient. We can show that $\widetilde{\theta}$ is asymptotically equivalent to a profiled GMM estimator that uses the optimal least favorable smoothing method, that is, let $\widetilde{\theta}_P = \arg\min_{\theta\in\Theta} \left\| M_T(\theta, \widehat{g}_\theta) \right\|_S^2$, where $\widehat{g}_\theta$ is essentially the local GMM smoother that treats all the parameters θ as known. We give more detail on this question in the Appendix. Our two step approach is very convenient from a computational point of view.

We discuss here our choice of GMM estimator. The optimal weight matrix for the unconditional moment restriction implied by a given set of instruments where the function g is known is $S_{opt} = \left(\text{var}\left(M_T(\theta, g_0) \right) \right)^{-1}$, which corresponds to using the particular set of instruments $z_{t-1} = (\partial \lambda_t^\intercal / \partial \theta) \Lambda_t^{-1} \Omega$, as in Cipollini and Gallo (2025) (when ζ_t is i.i.d.). This involves in our case a combination of all the past values of ℓ_{t-1}^*. However, this efficiency argument is not correct in our case for two reasons. First, it does not take into account of the nonparametric trend, which affects the semiparametric efficiency bound and hence the optimal instruments or weighting matrix. Second, we are assuming the MDS assumption for $\zeta_t - i_N$, which implies more restrictions. The efficiency bound for the conditional moment restriction in this setting is not yet derived. In principle one can extend Newey (1994) to this case, but it looks challenging. Chen et al. (2025) is close, they derive the efficiency bound for the case where the information set is of finite length, i.e., the key process is Markov of some order.

4.2.2 Restricted GAP Models

We next discuss the estimation of the parameters of the restricted GAP models we discussed above. A generic way of doing this is to estimate the unrestricted model and then impose the linear restrictions derived above by the method of minimum distance, Rothenberg (1973). This is convenient for understanding the theory, but in practice the unrestricted model may have too many parameters to allow reliable estimation. In that case it is convenient to find single equation methods that involve far fewer parameters to estimate.

The GAPD Model. In the special case where we have no lagged index dynamics,

$\lambda_{it} = \omega_i + \beta_{ii}\lambda_{i,t-1} + \gamma_{ii}\ell^*_{i,t-1} + \delta_i^\intercal \ell^*_{w,t-1}$, we can define $\theta_i = (\beta_{ii}, \gamma_{ii}, \delta_i^\intercal)^\intercal$ and estimate these parameters by GMM from the residuals of the i^{th} equation

$$\rho^+_{it}(\theta_i, \widehat{g}) = z_{t-1} \otimes (\zeta_{it}(\theta_i, \widehat{g}) - 1),$$

where $\zeta_{it}(\theta_i, \widehat{g}) = \widehat{\ell}^*_{it}/\widehat{\lambda}_{it}(\theta_i, \widehat{g})$, that is, we estimate GMM for each asset separately. That is,

$$\widetilde{\theta}_i = \arg\min_{\theta\in\Theta} \left\| M_{Ti}(\theta, \widetilde{g}) \right\|_S^2, \quad M_{Ti}(\theta, g) = \frac{1}{T}\sum_{t=1}^{T} \rho^+_{it}(\theta_i, g).$$

The GAPC model. Suppose that $\beta_{ii} = \beta$ and $\gamma_{ii} = \gamma$, i.e., (11) holds. In this case we first estimate the parameters of the model for the index liquidity $\lambda_{w,t} = \omega^\dagger + A^\dagger \lambda_{w,t-1} + D^\dagger \ell^*_{w,t-1}$ as the conditional mean of $\ell^*_{w,t}$, i.e., define $\zeta_{wt}(\theta^\dagger, \widehat{g}) = \Lambda_{w,t}(\theta^\dagger, \widehat{g})^{-1}\widehat{\ell}^*_{w,t}$, where $\Lambda_{w,t}(\theta^\dagger, \widehat{g}) = \text{diag}\{\lambda_{w_1,t}(\theta^\dagger, \widehat{g}), \ldots, \lambda_{w_R,t}(\theta^\dagger, \widehat{g})\}$ and $\widehat{\ell}^*_{w,t} = W^\intercal \widehat{\ell}^*_t$. Then apply GMM to estimate the parameters $\theta^\dagger$ and define recursively for each t

$$\widehat{\lambda}_{w,t} = \widehat{\omega}^\dagger + \widehat{A}^\dagger \widehat{\lambda}_{w,t-1} + \widehat{D}^\dagger \widehat{\ell}^*_{w,t-1}.$$

We then estimate the model (11) by single equation GMM using the estimated values $\widehat{\lambda}_{w,t}$. One could go back and improve efficiency using system methods or at least average over the different estimates of β, γ.

4.2.3 Prediction Error Variance

Given estimates of the dynamic parameters and the trend we may further define the residuals $\widehat{\zeta}_t = (\widehat{\zeta}_{1t}, \ldots, \widehat{\zeta}_{Nt})^\intercal$, where $\widehat{\zeta}_t = \widehat{G}_t^{-1} \times \widehat{\Lambda}_t^{-1} \times \ell_t$ (where $\widehat{G}_t = \text{diag}(\widehat{g}_1(t/T), \ldots, \widehat{g}_N(t/T))$ and $\widehat{\Lambda}_t = \text{diag}(\widehat{\lambda}_{1t}, \ldots, \widehat{\lambda}_{Nt})$) or $\widehat{\zeta}_{it} = \ell_{it}/\widehat{g}_i(t/T)\lambda_{it}(\widehat{\theta}, \widehat{g})$. Likewise, we may define residuals based on the second round smoother, i.e., $\widetilde{\zeta}_t = (\widetilde{\zeta}_{1t}, \ldots, \widetilde{\zeta}_{Nt})^\intercal$. Under the assumption that $E(\zeta_t \zeta_t^\intercal | \mathcal{F}_{t-1}) - i_N i_N^\intercal = \Omega(t/T)$, we estimate $\Omega(u)$ by

$$\widehat{\Omega}(u) = \frac{1}{T}\sum_{t=1}^{T} K_h(u - t/T) \left(\widehat{\zeta}_t - i_N\right)\left(\widehat{\zeta}_t - i_N\right)^\intercal. \tag{26}$$

We further estimate the prediction error variance $\Sigma(u)$ by

$$\widehat{\Sigma}(u) = \frac{1}{T}\sum_{t=1}^{T} K_h(u - t/T)\widehat{\Lambda}_t \left(\widehat{\zeta}_t - i_N\right)\left(\widehat{\zeta}_t - i_N\right)^\intercal \widehat{\Lambda}_t.$$

We estimate the triangular matrix $P(u)$ by $\widehat{P}(u)$, which is defined from the Cholesky factorization of the prediction error variance matrix $\widehat{\Sigma}(u)$. We can estimate the coefficient matrices $\Theta_k(t/T)$ by

$$\widehat{\Theta}_k(t/T) := \widehat{G}(t/T)\widehat{\Phi}_k\widehat{\Lambda}_{t-k}\widehat{\Omega}^{1/2}((t-k)/T)\widehat{A}^{\intercal}, \tag{27}$$

where the estimates $\widehat{\Phi}_k$ are derived from $\widehat{\theta}$, while $\widehat{A}$ is obtained from the ICA procedure. Estimation of A is performed by maximizing mutual independence according to some criterion. We use the `FastICA` algorithm of Hyvarinen (1999), which uses a fixed-point iteration scheme that maximizes a measure of non-Gaussianity of the rotated components.

Likewise we can define $\widetilde{\Omega}(u)$, $\widetilde{\sigma}(u)$, $\widetilde{P}(u)$, and $\widetilde{\Theta}_k(t/T)$ using the second round smoother.

4.2.4 Model Selection

We have considered unrestricted and restricted dynamic models that have quite different parameter cardinalities. To compare them on the same basis we use the Andrews and Lu (2001) GMM model selection procedure, which is based on computing

$$\left\| M_T(\widehat{\theta}, \widehat{g}) \right\|_S^2 + (|\theta| \times \ln(T))/T, \tag{28}$$

where $|\theta|$ denotes the cardinality of the vector θ for a given model. An alternative approach is to test the linear restrictions of our model using the large sample theory presented next.

5 Large sample properties

HLW1 established the root-T consistency of the GMM estimators of θ in the univariate liquidity case along with the pointwise distribution of the nonparametric trend estimator, in their case local constant. HLW2 extend that theory to allow for known discontinuities in the trend functions. We make some assumptions.

Definition. *A triangular array process* $\{X_{t,T},\, t = 0, 1, 2, \ldots,\, T = 1, 2, \ldots\}$ *is said to be alpha mixing if*

$$\alpha(k) = \sup_{T \geq 1} \sup_{A \in \mathcal{F}_{-\infty}^{n},\, B \in \mathcal{F}_{n+k}^{\infty}} |P(AB) - P(A)P(B)| \to 0, \tag{29}$$

as $k \to \infty$, *where* $\mathcal{F}_{-\infty}^{n,T}$ *and* $\mathcal{F}_{n+k,T}^{\infty}$ *are two* σ*–fields generated by* $\{X_{t,T},\, t \leq n\}$ *and* $\{X_{t,T},\, t \geq n+k\}$ *respectively. We call* $\alpha(\cdot)$ *the mixing coefficient.*

We suppose that ℓ_t^* is locally stationary and alpha mixing. This can be shown to hold under the parameter restrictions provided ζ_t is itself locally stationary and mixing under some further technical conditions. For a locally stationary mean zero vector process $x_t(u)$, we define the long run variance matrix as

$$\text{lrvar}(x_t(u)) = \sum_{k=-\infty}^{\infty} E(x_t(u)x_{t-k}(u)^\intercal).$$

We first consider the nonparametric trend estimators.

ASSUMPTION A1. *We suppose that $g_{i,j}(.) \in \mathcal{G}$, where for $0 < c, C < \infty$*

$$\mathcal{G} = \left\{ g : g : [0,1] \to \mathbb{R}_+,\ g(x) \geq c,\ \left|g''(x)\right| \leq C \text{ for all } x \in (0,1),\ \text{and } g''_+(0), g''_-(1) \text{ exist} \right\}.$$

Define $||g|| = \left(\int_0^1 g(u)^2 du\right)^{1/2}$ for all $g \in \mathcal{G}$.

ASSUMPTION A2. *Suppose that $\{v_t\}$, where $v_t = \Lambda_t \zeta_t - i_N \in \mathbb{R}^N$, is a locally stationary alpha mixing sequence with $E(v_t) = 0$ and $E(|v_{it}|^{2+\delta}) \leq C < \infty$ for some $\delta > 0$ for $i = 1, 2 \ldots, N$ and $t = 1, 2, \ldots.$ such that*

$$\sum_{k=1}^{\infty} \alpha(k)^{\frac{\delta}{2+\delta}} < \infty.$$

ASSUMPTION A3. *Suppose that K is symmetric about zero with compact support $[-1, 1]$ such that $K(\pm 1) = 0$ and K is twice differentiable where K'' is continuous on $[-1, 1]$. Let $||K||_2^2 = \int_{-1}^1 K(s)^2 ds$, and $\mu_j(K) = \int_{-1}^1 s^j K(s) ds$, $j = 0, 1, 2$.*

Let $g(u) = (g_{1,1}(u), g_{1,2}(u), \ldots, g_{N,J}(u))^\intercal \in \mathbb{R}^{NJ}$, and likewise $\widehat{g}(u) = (\widehat{g}_{1,1}(u), \ldots, \widehat{g}_{N,J}(u))^\intercal$, $\widetilde{g}(u) = (\widetilde{g}_{1,1}(u), \ldots, \widetilde{g}_{N,J}(u))^\intercal$ and $g''(u) = (g''_{1,1}(u), \ldots, g''_{N,J}(u))^\intercal$, and let $G^\oplus(u) = \text{diag}\{g_{1,1}(u), g_{1,2}(u), \ldots, g_{N,J}(u)\}$. Furthermore, let $v_t^\oplus = (v_{1t}D_{1t}, v_{1t}D_{2t}, \ldots, v_{Nt}D_{Jt})^\intercal$ be the seasonally segmented error process whose elements are locally stationary with mean zero, and in the second case. Let $\Omega^\oplus(u) = \Omega(u) \otimes I_J$ and $\Xi(u) = \text{lrvar}(v_t^\oplus(u))$.

THEOREM 1. *Suppose that assumptions A1-A3 hold and that $h \to 0$ and $Th \to \infty$. Then for any $u \in [0, 1]$ as $T \to \infty$ with N fixed,*

$$\sqrt{Th}\left(\widehat{g}(u) - g(u) - h^2 b(u)\right) \Longrightarrow N\left(0, V(u)\right),$$

$$b(u) = \frac{1}{2}\mu_2(K) g''(u)\ ; \quad V(u) = ||K||^2 \times G^\oplus(u) \times \Xi(u) \times G^\oplus(u),$$

Suppose that $\widehat{\theta}$ is root-T consistent. Then,

$$\sqrt{Th}\left(\widetilde{g}(u) - g(u) - h^2 b(u)\right) \Longrightarrow N\left(0, V_0(u)\right),$$

$$b(u) = \frac{1}{2}\mu_2(K)g''(u) \; ; \quad V_0(u) = ||K||^2 \times G^{\oplus}(u) \times \Omega^{\oplus}(u) \times G^{\oplus}(u).$$

The individual elements $\widehat{g}_{i,j}(u)$ have asymptotic variance $V_{ii}(u) = ||K||^2 \times g^2_{i,j}(u) \times \text{lrvar}(v_{it}(u)D_{jt})$ consistent with the univariate theory. In the event that ζ_t is i.i.d. and λ_t is strictly stationary, $\Xi(u) = \Xi$ does not depend on u. The pointwise limiting distributions of the common trend, idiosyncratic trend, and seasonal trend all follow because asymptotically they are linear combinations of all of the $\widehat{g}_{i,j}(u)$. We may wish to test the hypothesis

$\mathbf{H}_0^{NS}$: No seasonal effects, $g_{i,1}(u) = \ldots = g_{i,J}(u)$ for given i or for all i.

We may also wish to test the hypothesis that the trends are equal across units:

$\mathbf{H}_0^{ET}$: Equal trends, $g_{1,j}(u) = \ldots = g_{N,j}(u)$ for given j or for all j.

These hypotheses can be expressed as linear restrictions on the vector $g(u)$, that is, we can write the null hypotheses as $Qg(u) = 0$ for some r by NJ matrix Q, and so under the null hypothesis we have

$$\sqrt{Th}Q\widetilde{g}(u) \Longrightarrow N\left(0, QV_0(u)Q^{\intercal}\right).$$

Furthermore, the Wald test satisfies

$$Th\widetilde{g}(u)^{\intercal}Q^{\intercal}\left(Q\widetilde{V}_0(u)Q^{\intercal}\right)^{-1}Q\widetilde{g}(u) \Longrightarrow \chi^2(N-1), \tag{30}$$

where $\widetilde{V}_0(u) = ||K||^2\widetilde{G}^{\oplus}(u)\widetilde{\Omega}^{\oplus}(u)\widetilde{G}^{\oplus}(u)$.

We consider next the asymptotic properties of $\widehat{\omega}(u) = \text{vech}(\widehat{\Omega}(u))$ considered as an estimator of $\omega(u) = \text{vech}(\Omega(u))$. Let $\chi_t = \text{vech}((\zeta_t - i_N)(\zeta_t - i_N)^{\intercal} - \Omega(t/T))$ and let $H(u) = \text{lrvar}(\chi_t(u))$.

THEOREM 2. *Suppose that assumptions A1-A3 hold and that $h \to 0$ and $Th \to \infty$. Suppose that $\widehat{\theta}$ is root-T consistent. Suppose that the process χ_t is mean zero, locally stationary and mixing. Then, for any $u \in [0,1]$ as $T \to \infty$ with N fixed,*

$$\sqrt{Th}\left(\widehat{\omega}(u) - \omega(u) - h^2 b_\omega(u)\right) \Longrightarrow N\left(0, V_\omega(u)\right),$$

$$b_\omega = \frac{1}{2}\mu_2(K)\omega''(u) \; ; \quad V_\omega(u) = ||K||^2 \times H(u).$$

The asymptotic covariance matrix here does not depend on previous estimations but depends on the long run variance of χ_t. We may use this result to test for the constancy of $\omega(u)$ with respect to time.

THEOREM 3. *Suppose that Assumptions A1-A3 hold and that A4-A6 of HLW hold. We then have that*

$$\sqrt{T}\left(\widehat{\theta}-\theta_0\right) \Longrightarrow N(0,\Omega_\theta),$$
$$\Omega_\theta = \left(\Gamma_1^\intercal S\Gamma_1\right)^{-1}\Gamma_1^\intercal S V_1 S\Gamma_1\left(\Gamma_1^\intercal S\Gamma_1\right)^{-1},$$

where V_1 is the asymptotic variance of $\sqrt{T}M_T(\theta_0,\widehat{g})$, and

$$\Gamma_1 = \lim_{T\to\infty} E\left(\frac{\partial M_T(\theta_0,g_0)}{\partial\theta^\intercal}\right).$$

Furthermore,

$$\sqrt{T}\left(\widetilde{\theta}-\theta_0\right) \Longrightarrow N(0,\Omega_\theta^+),$$
$$\Omega_\theta^+ = \left(\Gamma_1^\intercal S\Gamma_1\right)^{-1}\Gamma_1^\intercal S V_1^+ S\Gamma_1\left(\Gamma_1^\intercal S\Gamma_1\right)^{-1},$$

where V_1^+ is the asymptotic variance of $\sqrt{T}M_T(\theta_0,\widetilde{g})$.

In particular, we show that

$$\sqrt{T}M_T(\theta_0,\widetilde{g}) = \frac{1}{\sqrt{T}}\sum_{t=1}^{T}\psi_t(\theta_0,g_0)+o_P(1)$$

where $\psi_t(\theta_0,g_0) = \left(z_{t-1}\otimes(\zeta_t-i_N)+\overline{F}_t(\zeta_t-i_N)\right)$, where

$$\overline{F}_t = E\left(\left(z_{t-1}i_N^\intercal\otimes I_N\right)\left(I_N-\sum_{j=0}^{\infty}\left(\ell_{t-1-j}^{*\intercal}\otimes\Lambda_t^{-1}\Psi_N^\intercal B^j\Gamma\right)\right)\right)\Psi_N^\intercal. \tag{31}$$

We can obtain standard errors by calculating the short run variance of $\psi_t(\widetilde{\theta},\widetilde{g})$. The key point here is that the estimation of the nonparametric trend has a consequence on the variance of the dynamic parameter estimators and this should be taken into account when conducting inference.

6 Empirical study: Country ETFs

In this section, we apply the MARSLiQ model to analyze a sample of ETFs from the G7 countries, Australia and Hong Kong.[2] The sample period ranges from October 1996 to

[2]Our sample includes the SPDR S&P 500 ETF Trust and the iShares MSCI ETFs for the United Kingdom, France, Germany, Japan, Canada, Italy, Australia and Hong Kong.

October 2025. In the All Country World Index (ACWI), these nine countries collectively represent 82.32% of the total index market capitalization. The breakdown is as follows: the United States (63.19%), Japan (5.48%), United Kingdom (3.41%), Canada (3.02%), France (2.32%), Germany (2.05%), Australia (1.66%), Italy (0.70%)and Hong Kong (0.49%).

6.1 Long-run illiquidty trends

We estimate the individual long-run trend functions allowing for potential seasonal patterns in the illiquidity trend and we focus on the day-of-the-week effect, which has been documented for the U.S. stock market in the literature; see e.g. Chordia et al. (2005) and Hameed et al. (2010). Specifically, for each asset i and weekday j, we estimate $g_{i,j}(u)$ using a local linear estimator as specified in (22) and we then construct $G_t = \prod_{j=1}^{J} \text{diag}\left(g_{1,j}(t/T)^{D_{jt}}, \ldots, g_{N,j}(t/T)^{D_{jt}}\right)$ which can be used to compute the detrended series, i.e. $\widehat{\ell}_t^* = \widehat{G}_t^{-1}\ell_t$. As in the univariate case, after estimating the dynamic parameters of the λ_t process, we can obtain the prewhitened illiquidity $\ell_{it}^\dagger = \ell_{it}/\lambda_{it}$ that is purged of the short-run variation. Similarly, we estimate $g_{i,j}(u)$ using the local linear kernel smoother to obtain an improved estimator of $\tilde{g}_{i,j}(u)$. Additionally, we construct the common trend which is the weighted average of $g_{i,j}(u)$ as defined in (23). This allows us to further define the country-specific trends and the time-varying global seasonal components.

In Figure 1, we plot the log of the trend function of the illiquidity series, i.e., $\log \tilde{G}(t/T)$, which includes the day-of-the-week seasonal effect.[3] The US and Japanese ETFs are the most liquid over the whole sample, while other countries experience changes in their relative ranking over time. The ETFs for Australia, Canada and UK are less liquid before 2000, but most European ETFs experience an increase in illiquidity relative to others with the successive Global Financial Crisis (GFC) and Euro area crisis. While these effects seem to dissipate after 2015 for Germany and the UK, the French and Italian ETFs remain less liquid compared to others throughout the rest of the sample.

[3]We plot the logarithm of the trends to illustrate their time variation more clearly, although we model illiquidity directly and estimate its trend in levels. The estimated trends are plotted in Figure 9 of the appendix.

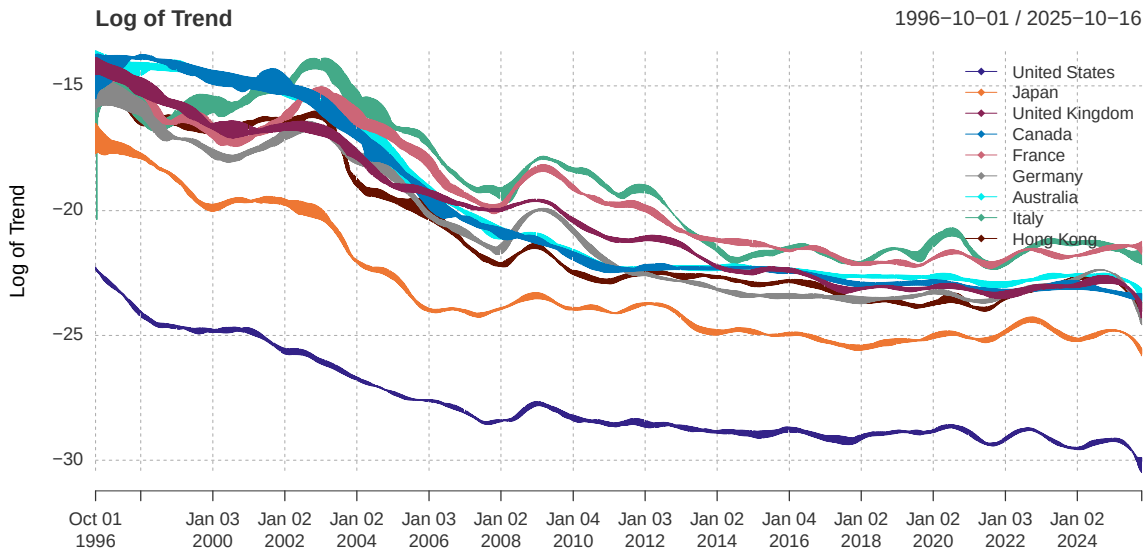

Figure 1: Log of illiquidity trends.

6.1.1 Common trend

Figure 1 clearly shows that all series move closely together, indicating the presence of a global trend that captures the overall long-term improvement in liquidity conditions and stress episodes during major adverse events in global markets. Thus, we construct the common trend as a weighted sum of normalized individual trend functions, i.e., $\widetilde{g}_0(u) = \sum_{i=1}^{N}\sum_{j=1}^{J}\vartheta_{i,j}\widetilde{g}_{i,j}(u)$. For the weighting scheme, we consider both equal-weighted and market-cap-weighted schemes between countries and simple equal weights among different weekdays. The resulting series are displayed in Figure 2.

There is a clear overall downward trend in the illiquidity series before the GFC, which corresponds to improved liquidity conditions. Between 2000 and 2003, several countries exhibit a moderate increase in illiquidity, which may reflect deteriorating liquidity following the burst of the dot-com bubble. Around the GFC, there is a significant increase in illiquidity across most markets. Afterwards, the illiquidity process fluctuates at a more stable level with some temporary spikes – indicating worsening liquidity conditions – around the Covid pandemic and at the start of the monetary policy tightening phase towards the end of 2021.

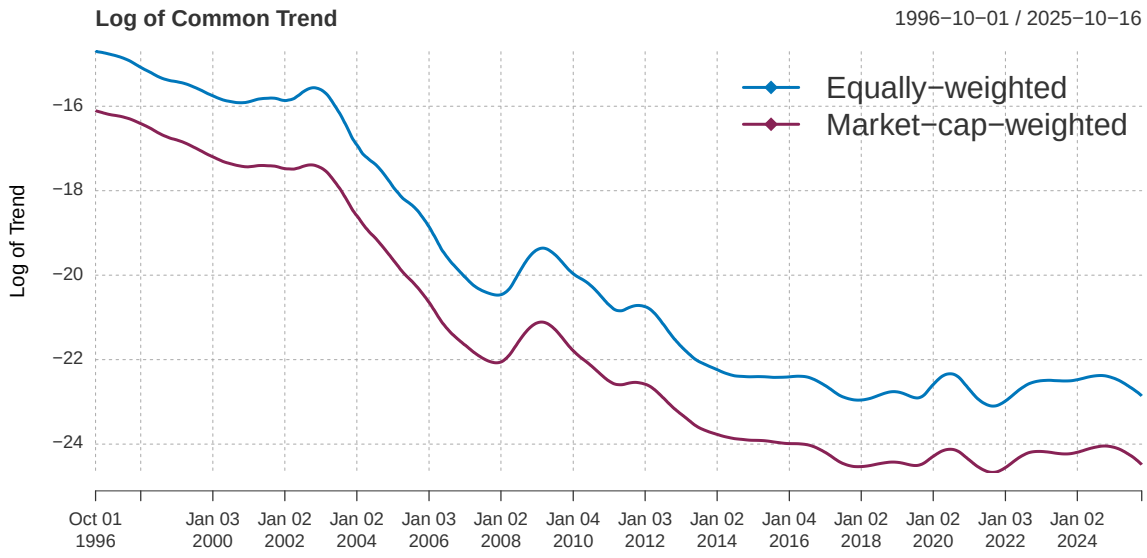

Figure 2: Log of the common trend.

6.1.2 Country-specific trends

Figure 3 plots the log of country-specific illiquidity trends, defined as the weighted average of trends $g_{i,j}(u)$ over all seasons scaled by the common trend, i.e., $\widetilde{g}_i^{\&}(u) = \sum_{j=1}^{J} \psi_j \frac{\widetilde{g}_{i,j}(u)}{\widetilde{g}_0(u)}$. Shaded areas indicate recession periods. These relative trends reflect deviations from the global liquidity factor and capture variations in idiosyncratic liquidity conditions. The United States consistently shows the lowest illiquidity trend, indicating the highest liquidity, while Italy exhibits the highest trend level overall, suggesting persistently poor liquidity conditions in its stock market. Several countries exhibit increases in illiquidity ahead or at the beginning of domestic economic recessions, in line with empirical evidence on the strong relation between stock market liquidity and the business cycle (Næs et al. (2011)). For example, France, Germany, and Italy show pronounced spikes in the early 2000s, a period marked by economic vulnerabilities and rising interest rates in the euro area. The UK exhibits periods of elevated illiquidity between 2008 and 2013, which roughly aligns with the period ranging from the start of the GFC to the end of the Euro Area crisis. The rise in illiquidity after 2022 is most evident in the UK and other European countries, likely driven by the sharp tightening in the monetary policy stance, energy market disruptions, and renewed concerns over fiscal and sovereign risk.

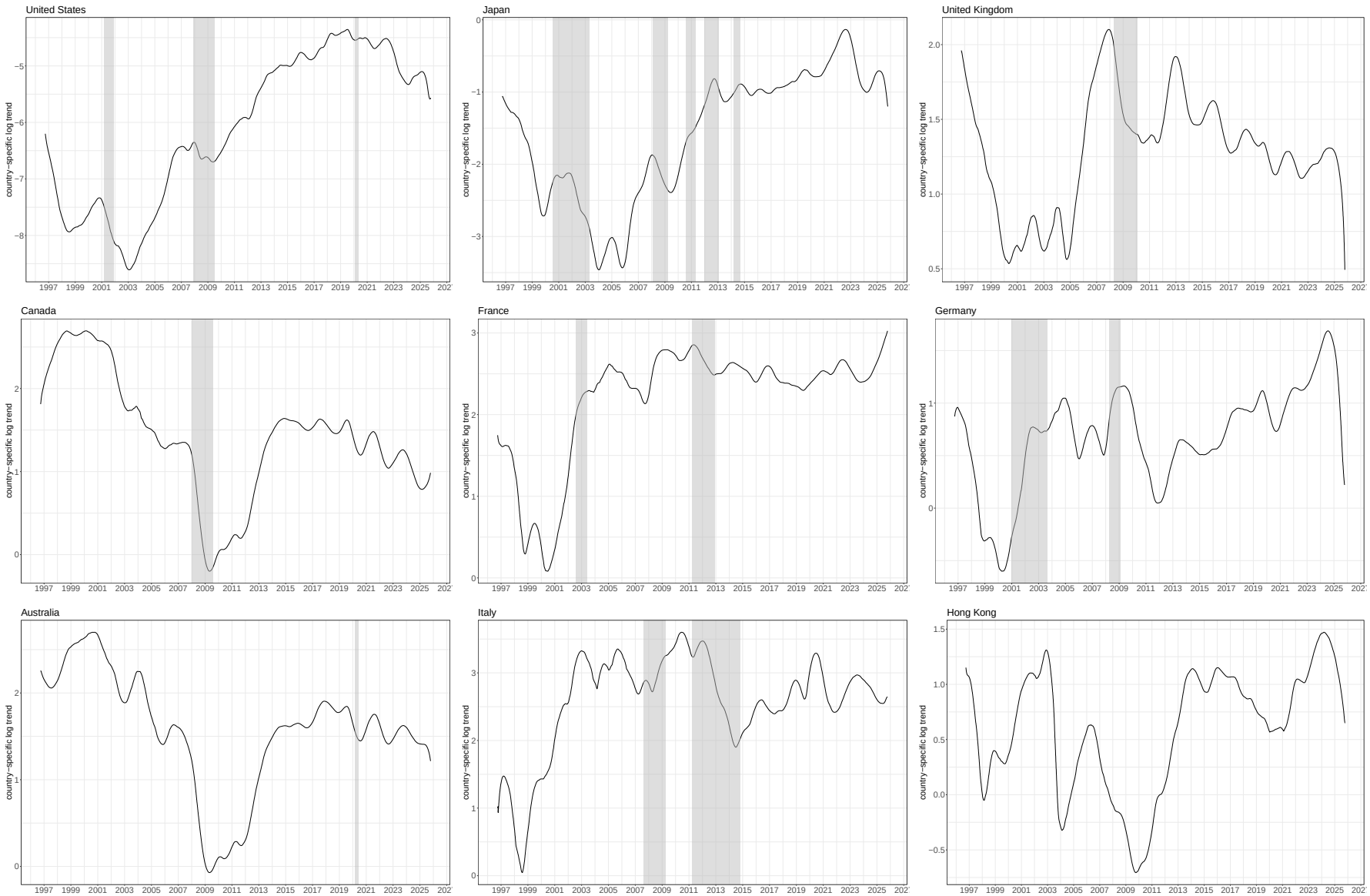

Figure 3: Log of country-specific trends. Shaded areas correspond to recession periods of each country.

6.1.3 Global seasonal trends

Figure 4 plots the log of time-varying global seasonal illiquidity trends, defined as the weighted average of trends $g_{i,j}(u)$ over all countries scaled by the common trend, i.e., $\widetilde{g}_j^{\%}(u) = \sum_{i=1}^{N} \tau_i \frac{\widetilde{g}_{i,j}(u)}{\widetilde{g}_0(u)}$. We observe substantial variation in the seasonal component over time, along with noticeable differences across weekdays at any given point. Liquidity generally deteriorates around weekends, i.e., on Mondays and Fridays, while it tends to improve on Tuesdays. The liquidity level on Wednesdays shows particularly pronounced fluctuations over time. This pattern could be explained by the fact that macroeconomic announcements such as monetary policy decisions by major central banks tend to take place on Wednesdays and Thursdays. These announcements could result in worsened liquidity conditions as market participants try to limit their exposure to incoming news shocks.

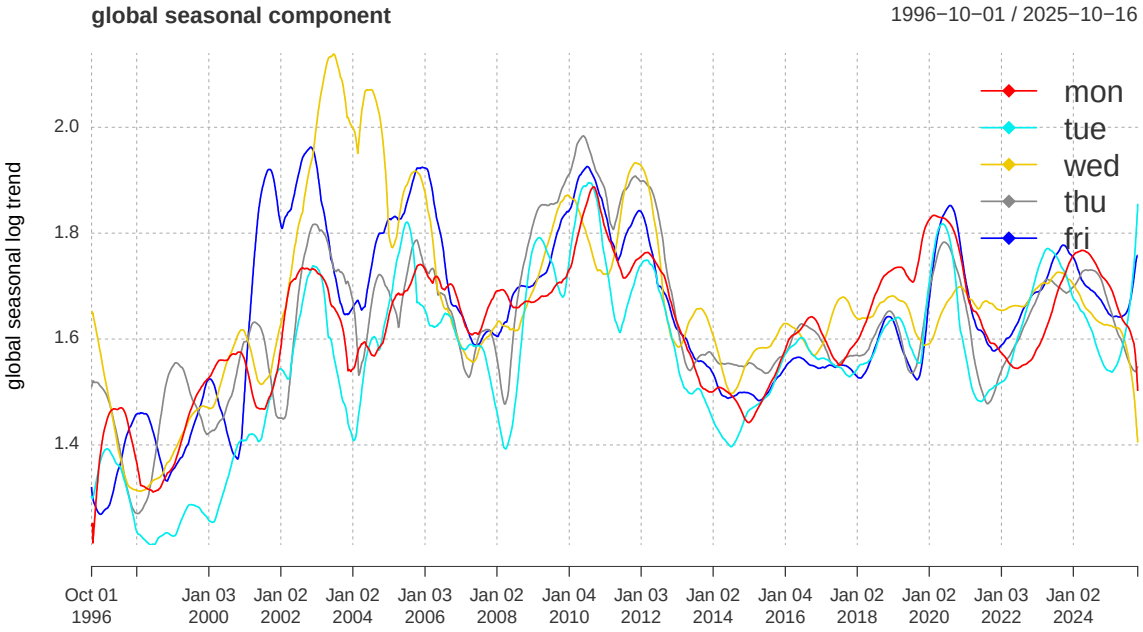

Figure 4: Time-varying global seasonal component.

6.2 Short-run illiquidity dynamics

We obtain the detrended illiquidity series for country i, $\widetilde{\ell}_t^* = (\widetilde{\ell}_{1t}^*, \ldots, \widetilde{\ell}_{Nt}^*)^\intercal$, where $\widetilde{\ell}_{it}^* = \ell_{it}/\widetilde{g}_i(t/T)$. Based on the conditional moment restriction $E(\zeta_t|\mathcal{F}_{t-1}) = i_N$, we can estimate the dynamic parameters θ for the short-run illiquidity process λ_t using a GMM approach.

We start with the special case where $B = D_B$ is a diagonal matrix, which can be estimated using single equation methods. We focus on two scenarios: first, we consider the GARPD model with the parameter matrix decomposition $\Gamma = D_\Gamma + D^* W^\top$ where W contains both equally-weighted and market-cap-weighted schemes. This specification yields four parameters to characterize the dynamics for each country.[4] Second, we estimate Γ matrix directly, which is more flexible but requires estimating $N+1$ parameters for every country.

Table 1: Estimates of the λ_t process parameters in the special case of $B = D_B$ using single equation method.

	D_{Bii}	$D_{\Gamma ii}$	D^*_{i1}	D^*_{i2}	B										Γ									ω
Combine																								
United States	0.725	0.036	0.002	0.121	0.725										0.130	0.008	0.005	0.005	0.004	0.003	0.003	0.001	0.001	0.116
Japan	0.764	0.152	0.052	-0.010		0.764									-0.002	0.157	0.005	0.005	0.005	0.005	0.006	0.006	0.006	0.044
United Kingdom	0.646	0.155	0.106	-0.073			0.646								-0.044	0.007	0.163	0.009	0.010	0.010	0.010	0.011	0.011	0.166
Canada	0.744	0.156	0.103	0.026				0.744							0.032	0.013	0.013	0.169	0.012	0.012	0.012	0.012	0.012	-0.029
France	0.623	0.126	0.176	-0.079					0.623						-0.041	0.014	0.016	0.017	0.144	0.018	0.018	0.019	0.019	0.154
Germany	0.767	0.127	0.096	-0.053						0.767					-0.030	0.007	0.009	0.009	0.009	0.137	0.010	0.010	0.010	0.062
Australia	0.823	0.118	0.069	-0.025							0.823				-0.011	0.006	0.007	0.007	0.007	0.007	0.125	0.007	0.008	0.015
Italy	0.625	0.124	0.202	-0.098								0.625			-0.053	0.016	0.018	0.019	0.020	0.020	0.020	0.145	0.022	0.147
Hong Kong	0.708	0.163	0.090	-0.004									0.708		0.007	0.010	0.010	0.010	0.010	0.010	0.010	0.010	0.173	0.043
Estimate Γ																								
United States					0.720										0.129	0.005	0.011	0.007	-0.002	0.001	0.001	0.002	0.007	0.120
Japan						0.686									-0.027	0.178	-0.013	0.016	0.008	0.009	0.009	0.001	0.020	0.113
United Kingdom							0.654								-0.060	0.013	0.163	0.004	0.006	0.012	0.018	0.005	0.017	0.168
Canada								0.708							0.053	0.004	0.009	0.182	0.025	-0.002	0.023	0.012	0.018	-0.033
France									0.623						-0.028	0.019	0.006	0.017	0.137	0.035	0.016	0.026	-0.001	0.149
Germany										0.763					-0.017	-0.001	0.011	0.009	0.002	0.140	0.010	0.015	0.012	0.056
Australia											0.810				-0.026	0.002	0.001	0.011	0.003	0.016	0.131	0.006	0.008	0.038
Italy												0.623			-0.061	0.016	0.038	0.028	0.007	0.006	0.026	0.147	0.005	0.164
Hong Kong													0.666		-0.046	0.024	-0.005	0.024	0.007	0.016	0.010	0.009	0.176	0.119

Note: Under the restriction that the B matrix is diagonal, we carry out the estimation line by line.

We reconstruct the B and Γ matrices from the estimated parameters and the largest eigenvalue of the matrix $B + \Gamma$ is below one in both specifications indicating that the λ_t process is strictly stationary. Across countries, the autoregressive coefficient D_{Bii} is generally moderate to high and the diagonal elements of the estimated Γ matrix are of larger magnitude than the off-diagonal ones. This indicates that country i's short-run illiquidity is primarily driven by its own lagged value and past detrended illiquidity. The spillover effects in the first specification are captured by the two short-run liquidity indices—one equally weighted and one market-cap based dominated by the US which accounts for 77% of the total market capitalization. In the second specification, spillovers are reflected

[4] We also consider the cases where W contains equal weights or market-cap based weights separately. Results reported in Table 4 of the appendix suggest that considering a single weighting scheme might be too restrictive to fully capture the dynamics.

by the off-diagonal elements of the estimated Γ matrix. Notably, the entries Γ_{i1} for $i = 2, \ldots, N$ are mostly negative with values ranging from -0.053 to -0.002 and from -0.061 to -0.017 respectively. This suggests that US liquidity conditions have a relatively large and overall negative effect on the short-term liquidity of other countries. A notable exception is Canada, whose short-term liquidity is positively impacted by US liquidity conditions.

We further elaborate on model selection for empirical applications by considering two groups of models where we estimate the parameter matrices for the panel of countries jointly. In the first group, we estimate the parameter matrices B and Γ directly, with three specifications: both matrices unrestricted, B diagonal with unrestricted Γ, and Γ diagonal with unrestricted B. In the second group, we consider the GAP model structure where the parameter matrices are decomposed as $B = D_B + B^* W^\top, \quad \Gamma = D_\Gamma + D^* W^\top$. Here, W denotes the weighting scheme, taken as equal-weighting, market-cap weighting, or a combination of the two.[5]

Table 2: Andrews and Lu (2001) GMM model selection.

	unrestricted	diag Γ	diag B	W_{EQ}	W_{MCap}	W_{Combine}
k	162	90	90	36	36	54
$\text{T}\|M_T\|_S^2$	10.4638	50.3979	21.6047	31.4823	41.0442	26.6724
AIC	0.0458	0.0315	0.0276	0.0142	0.0155	0.0184
BIC	0.1987	0.1165	0.1126	0.0482	0.0495	0.0694

Note: W_{EQ} and W_{MCap} denote the equal-weighted and market-capitalization weighting schemes, respectively. $W_{\text{Combine}} = (W_{\text{EQ}}, W_{\text{MCap}})$ which incorporates both schemes.

We compute the AIC and BIC for model selection as proposed in Andrews and Lu (2001) to compare the empirical fit of restricted and unrestricted models and report the results in Table 2. Within the first group of models, the preferred specification is the one with diagonal B which achieves the best trade-off between fit and parsimony. Additionally, this restriction allows for estimation by single-equation methods, as the process λ_{it} depends only on its own lag and on the lagged detrended illiquidity series ℓ_t^* which are constructed by rescaling the illiquidity series using the estimated trend function. Within the GAP models, using a combination of the two weighting schemes improves the empirical fit compared to each scheme. However, the resulting increase in the number of estimated parameters

[5]The estimates for the two groups of models are reported in Table 5 and Table 6 of the appendix respectively.

more than offset this effect and leads to a worsening in the information criteria. The equal-weighted scheme provides a better fit to the data compared to the market-capitalization one. Overall, the GAP models outperform the first group of models in terms of information criteria, which confirms the tractability of this specification and prefigures interesting opportunities to scale the application of liquidity modeling to larger asset systems.

6.3 Variance decomposition and connectedness

After obtaining the estimates of the B and Γ matrices, we construct the connectedness table using the forecast error variance decomposition described in Section 3.2. We focus on the model specification with diagonal B and unrestricted Γ. Table 3 reports the full-sample connectedness measures for the liquidity series of different countries, based on Independent Component Analysis (ICA), which exploits non-Gaussian features of our data. The (i, j)-th entry in the table represents the estimated contribution of shocks from country j to the forecast error variance of country i. The row sums of the off-diagonal elements—the "FROM" column—indicate the contributions received from other countries, while the column sums of the off-diagonal elements—the "TO" row—reflect the contributions made to other countries. "NET" is defined as "TO" minus "FROM".

For both the 1-day and 22-day horizons, US is the dominant transmitter of shocks, with the highest "NET" contributions (94.79% and 101.81% at the 1-day and 22-day horizons, respectively), reflecting its high contribution to other countries' variation in liquidity. This contribution is particularly concentrated in European countries such as UK, France and Germany. In contrast, countries such as Japan, Canada, Australia, Italy, and Hong Kong exhibit lower levels of cross-country spillovers, with limited transmission to others. Lastly, the Spillover Index (SI), defined as the share of total forecast error variance attributed to cross-country spillovers, is approximately 28.01% and 31.24% for the 1-day and 22-day horizons, respectively, indicating that around a third of liquidity forecast variance arises from foreign shocks. In addition, Figure 5 shows the spillover index across forecasting horizons of up to roughly three months. The index rises rapidly during the first month, reaching near its maximum, and then increases only gradually thereafter.

Data suggests that the covariance matrix could be time-varying and we estimate $\Omega(t/T)$

Table 3: Full-sample connectedness table (ICA).

	United States	Japan	United Kingdom	Canada	France	Germany	Australia	Italy	Hong Kong	FROM
1 day ahead										
United States	55.75	0.09	43.13	0.13	0.05	0.05	0.14	0.03	0.63	44.25
Japan	7.70	88.60	0.33	0.20	0.03	0.47	1.72	0.02	0.94	11.40
United Kingdom	44.40	0.96	24.43	0.04	21.14	8.26	0.23	0.18	0.35	75.57
Canada	4.14	0.00	0.31	92.57	0.38	0.06	2.09	0.19	0.27	7.43
France	29.15	0.11	16.87	0.07	52.81	0.55	0.02	0.02	0.39	47.19
Germany	24.68	0.01	5.90	0.06	0.08	68.72	0.30	0.10	0.14	31.28
Australia	10.00	0.00	1.04	0.02	0.03	0.32	88.36	0.08	0.15	11.64
Italy	7.65	0.05	2.07	0.02	0.19	0.33	0.24	88.93	0.54	11.07
Hong Kong	11.34	0.01	0.19	0.00	0.04	0.17	0.36	0.15	87.75	12.25
TO	139.04	1.23	69.85	0.53	21.95	10.21	5.10	0.77	3.42	252.09
NET	94.79	-10.17	-5.73	-6.90	-25.25	-21.07	-6.54	-10.30	-8.84	SI=28.01%
22 day ahead										
	United States	Japan	United Kingdom	Canada	France	Germany	Australia	Italy	Hong Kong	FROM
United States	57.35	0.40	40.43	0.60	0.09	0.08	0.28	0.07	0.71	42.65
Japan	8.06	85.02	0.49	0.89	0.29	0.58	2.60	0.07	2.00	14.98
United Kingdom	43.15	1.07	25.91	0.15	20.46	7.71	0.81	0.20	0.55	74.09
Canada	9.28	0.53	0.58	82.93	0.48	0.09	4.03	0.45	1.64	17.07
France	29.53	0.31	17.74	0.68	49.86	0.58	0.52	0.35	0.42	50.14
Germany	25.08	0.06	7.78	0.94	0.07	64.30	0.62	0.29	0.86	35.70
Australia	9.60	0.02	2.44	1.48	0.04	0.73	84.76	0.20	0.73	15.24
Italy	8.25	0.23	3.92	0.94	0.17	0.36	0.88	84.23	1.01	15.77
Hong Kong	11.51	0.51	0.77	0.80	0.14	0.28	1.21	0.28	84.51	15.49
TO	144.45	3.11	74.15	6.49	21.73	10.40	10.95	1.92	7.92	281.12
NET	101.81	-11.87	0.05	-10.58	-28.40	-25.30	-4.29	-13.85	-7.57	SI=31.24%

Note: The (i, j)-th value is the estimated contribution to the variance forecast error of country i due to the shocks from county j. Specification of λ_t follows the special case with diagonal B and unrestricted Γ and the parameters are estimated using GMM.

using a local linear smoother. In this case, the spillovers would be varying over time and we plot the spillover index in Figure 6. The plot shows significant time variation in the magnitude of liquidity spillovers, underscoring the importance of accounting for time-varying interconnectedness in global markets. The index spikes sharply during the Global Financial Crisis (2008–2009), reflecting the rapid transmission of shocks across financial markets. A second wave of elevated spillovers follows during the European sovereign debt crisis (2009–2012), though with slightly smaller magnitude. The spillover index rises sharply over 2018-2019—a period marked by the initial phase of quantitative tightening by the Federal Reserve and a first escalation in the China-US trade tensions. This increase is followed by two consecutive peaks: during the market turmoil of the COVID pandemic in 2020, and during the global tightening in monetary policy in response to inflationary pres-

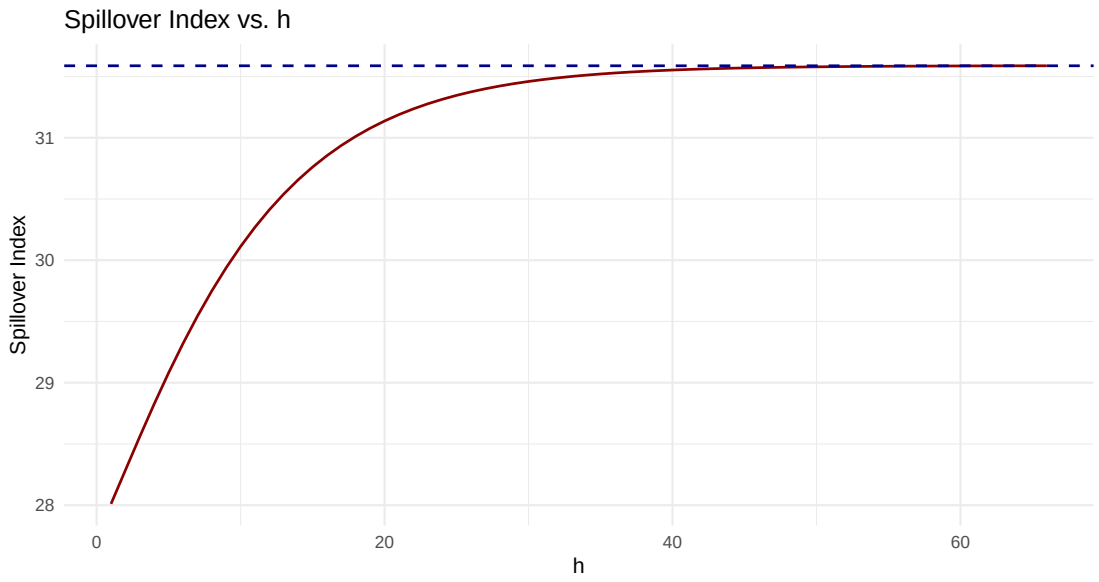

Figure 5: Spillover Index with respect to different horizons (ICA).

sures towards the end of 2021. Lastly, the spillover index progressively reaches its highest value in the sample during 2025. This pronounced increase in market liquidity spillovers is likely driven by a combination of factors, including the sharp market reaction globally following US tariff announcements, and rising concerns about sovereign debt sustainability across advanced economies.

Taken together, these patterns suggest that a wide range of factors can lead to an amplification of cross-country liquidity linkages and our framework provides a convenient summary indicator to identify them. Lastly, we also plot the spillover index constructed using the Cholesky and spectral decomposition in Figures 10 and 11 in the appendix. We note that although using different approaches leads to different detailed connectedness tables, the time variations of spillover indexes are quite consistent with each other.

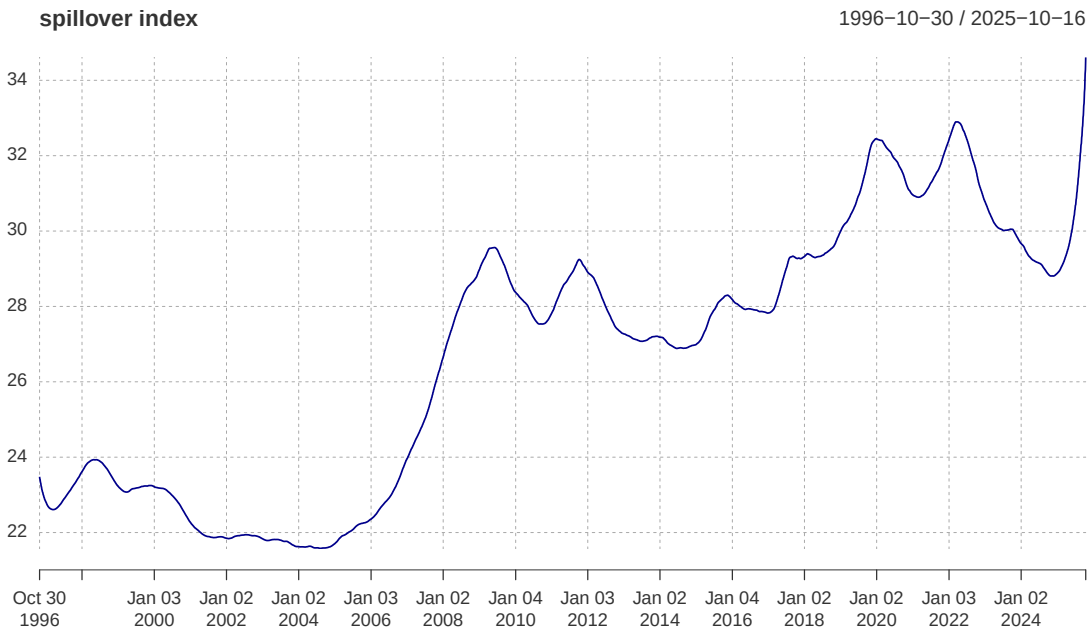

Figure 6: Spillover Index for horizon $h = 22$ (ICA).

References

Amihud, Y. (2002): "Illiquidity and stock returns: Cross-section and time-series effects". *Journal of Financial Markets* 5.1, pp. 31–56.

Andrews, D. W. and Lu, B. (2001): "Consistent model and moment selection procedures for GMM estimation with application to dynamic panel data models". *Journal of Econometrics* 101.1, pp. 123–164.

Barigozzi, M., Brownlees, C., Gallo, G. M. and Veredas, D. (2014): "Disentangling systematic and idiosyncratic dynamics in panels of volatility measures". *Journal of econometrics* 182.2, pp. 364–384.

Bauwens, L., Laurent, S. and Rombouts, J. V. (2006): "Multivariate GARCH models: a survey". *Journal of Applied Econometrics* 21.1, pp. 79–109.

Boussama, F. (1998): "Ergodicity, mixing and estimation in GARCH models". PhD thesis. Université Paris Diderot-Paris 7.

Brunnermeier, M. K. and Pedersen, L. H. (2009): "Market liquidity and funding liquidity". *The Review of Financial Studies* 22.6, pp. 2201–2238.

Chen, X., Liao, Y. and Wang, W. (2025): "Inference on time series nonparametric conditional moment restrictions using nonlinear sieves". *Journal of Econometrics* 249, p. 105920.

Chen, X., Linton, O. B. and Van Keilegom, I. (2003): "Estimation of semiparametric models when the criterion function is not smooth". *Econometrica* 71.5, pp. 1591–1608.

Chordia, T., Roll, R. and Subrahmanyam, A. (2000): "Commonality in liquidity". *Journal of Financial Economics* 56.1, pp. 3–28.

Chordia, T., Sarkar, A. and Subrahmanyam, A. (2005): "An empirical analysis of stock and bond market liquidity". *The Review of Financial Studies* 18.1, pp. 85–129.

Cipollini, F., Engle, R. F. and Gallo, G. M. (2013): "Semiparametric vector MEM". *Journal of Applied Econometrics* 28.7, pp. 1067–1086.

Cipollini, F., Engle III, R. F. and Gallo, G. M. (2006): *Vector multiplicative error models: representation and inference.*

Cipollini, F. and Gallo, G. M. (2025): "Multiplicative Error Models: 20 years on". *Econometrics and Statistics* 33, pp. 209–229.

Dahlhaus, R. (1997): "Fitting time series models to nonstationary processes". *The Annals of Statistics* 25.1, pp. 1–37.

Diebold, F. X. and Yilmaz, K. (2014): "On the network topology of variance decompositions: Measuring the connectedness of financial firms". *Journal of Econometrics* 182.1. Causality, Prediction, and Specification Analysis: Recent Advances and Future Directions, pp. 119–134.

Engle, R. (2002): "New frontiers for ARCH models". *Journal of Applied Econometrics* 17.5, pp. 425–446.

Engle, R. F. and Campos-Martins, S. (2023): "What are the events that shake our world? Measuring and hedging global COVOL". *Journal of Financial Economics* 147.1, pp. 221–242.

Engle, R. F. and Rangel, J. G. (2008): "The spline-GARCH model for low-frequency volatility and its global macroeconomic causes". *The Review of Financial Studies* 21.3, pp. 1187–1222.

Fan, J and Gijbels, I. (1996): *Local polynomial modelling and its applications*. Chapman and Hall.

Francisco-Fernández, M., Vilar-Fernández, J. M. and Vilar-Fernández, J. A. (2003): "On the uniform strong consistency of local polynomial regression under dependence conditions". *Communications in Statistics-Theory and Methods* 32.12, pp. 2415–2440.

Hafner, C. M., Herwartz, H. and Maxand, S. (2022): "Identification of structural multivariate GARCH models". *Journal of Econometrics* 227.1. Annals Issue: Time Series Analysis of Higher Moments and Distributions of Financial Data, pp. 212–227.

Hafner, C. M. and Linton, O. B. (2010): "Efficient estimation of a multivariate multiplicative volatility model". *Journal of Econometrics* 159.1, pp. 55–73.

Hafner, C. M., Linton, O. B. and Wang, L. (2024): "Dynamic Autoregressive Liquidity (DArLiQ)". *Journal of Business & Economic Statistics* 42.2, pp. 774–785.

Hafner, C. M., Linton, O. B. and Wang, L. (2025): "The permanent and temporary effects of stock splits on liquidity in a dynamic semiparametric model". *Journal of Business & Economic Statistics* Accepted, pp. 1–25.

Hameed, A., Kang, W. and Viswanathan, S. (2010): "Stock market declines and liquidity". *The Journal of Finance* 65.1, pp. 257–293.

Hasbrouck, J. and Seppi, D. J. (2001): "Common factors in prices, order flows, and liquidity". *Journal of Financial Economics* 59.3, pp. 383–411.

Herwartz, H. and Plödt, M. (2016): "The macroeconomic effects of oil price shocks: Evidence from a statistical identification approach". *Journal of International Money and Finance* 61, pp. 30–44.

Hyvarinen, A. (1999): "Fast and robust fixed-point algorithms for independent component analysis". *IEEE Transactions on Neural Networks* 10.3, pp. 626–634.

Knight, M. I., Nunes, M. and Nason, G. (2016): "Modelling, detrending and decorrelation of network time series". *arXiv preprint arXiv:1603.03221*.

Lütkepohl, H. (2005): *New Introduction to Multiple Time Series Analysis*. Springer-Verlag Berlin Heidelberg.

Næs, R., Skjeltorp, J. A. and Ødegaard, B. A. (2011): "Stock market liquidity and the business cycle". *The Journal of Finance* 66.1, pp. 139–176.

Nason, G., Salnikov, D. and Cortina-Borja, M. (2025): "Generalized network autoregressive modelling of longitudinal networks with application to presidential elections in the USA". *arXiv preprint arXiv:2503.10433*.

Newey, W. K. (1994): "The asymptotic variance of semiparametric estimators". *Econometrica: Journal of the Econometric Society*, pp. 1349–1382.

Pesaran, H. and Shin, Y. (1998): "Generalized impulse response analysis in linear multivariate models". *Economics Letters* 58.1, pp. 17–29.

Rothenberg, T. J. (1973): *Efficient estimation with a priori information*. Yale University Press.

Sims, C. A. (1980): "Macroeconomics and Reality". *Econometrica* 48.1, pp. 1–48.

A Theoretical Calculations

A.1 Local Stationary case

Here, we establish an expression for the matrices $E\left(\lambda_t\lambda_t^\intercal\right)$ and $E\left(\lambda_t\lambda_t^\intercal\right) - i_N i_N^\intercal$ in the case where $\zeta_t - i_N$ is a locally stationary martingale difference sequence with mean zero and unconditional variance $\Omega(t/T)$ also here denoted Ω_t.

We can write the dynamic equation as

$$\lambda_t = i_N + (B+\Gamma)(\lambda_{t-1} - i_N) + \Gamma\Lambda_{t-1}(\zeta_{t-1} - i_N)$$

since $\omega = \left(I_N - (B+\Gamma)\right) i_N$. Taking expectations of the outer product we obtain

$$\begin{aligned} E\left((\lambda_t - i_N)(\lambda_t - i_N)^\intercal\right) &= (B+\Gamma)\, E\left((\lambda_{t-1} - i_N)(\lambda_{t-1} - i_N)^\intercal\right)(B+\Gamma)^\intercal + \Gamma E\left(\Lambda_{t-1}\Omega_{t-1}\Lambda_{t-1}\right)\Gamma^\intercal \\ &= (B+\Gamma)\, E\left((\lambda_{t-1} - i_N)(\lambda_{t-1} - i_N)^\intercal\right)(B+\Gamma)^\intercal + \Gamma\Omega_{t-1}\Gamma^\intercal \\ &\quad + \Gamma E\left((\Lambda_{t-1} - I_N)\,\Omega_{t-1}\,(\Lambda_{t-1} - I_N)^\intercal\right)\Gamma^\intercal, \end{aligned}$$

since the cross products are mean zero. We write

$$\operatorname{vec}\left(E\left((\lambda_t - i_N)(\lambda_t - i_N)^\intercal\right)\right) = E\left((\lambda_t - i_N)\otimes(\lambda_t - i_N)\right).$$

We have

$$\begin{aligned} E\left((\lambda_t - i_N)\otimes(\lambda_t - i_N)\right) &= \left((B+\Gamma)\otimes(B+\Gamma)\right) E\left((\lambda_{t-1} - i_N)\otimes(\lambda_{t-1} - i_N)\right) + (\Gamma\otimes\Gamma)\operatorname{vec}(\Omega_{t-1}) \\ &\quad + (\Gamma\otimes\Gamma)\, E\left((\Lambda_{t-1} - I_N)\otimes(\Lambda_{t-1} - I_N)\right)\operatorname{vec}(\Omega_{t-1}). \end{aligned}$$

This is a difference equation. Since we suppose that the process $\zeta_t - i_N$ is locally stationary, we expect that $\psi(u) = E\left((\lambda_t - i_N)\otimes(\lambda_t - i_N)\right) \simeq E\left((\lambda_{t-1} - i_N)\otimes(\lambda_{t-1} - i_N)\right)$ for $u = t/T$. Notice further that for $\Lambda_t = \operatorname{diag}\{\lambda_t\}$ we have

$$E\left((\Lambda_t - I_N)\otimes(\Lambda_t - I_N)\right) = E\left(\operatorname{diag}\{(\lambda_t - i_N)\otimes(\lambda_t - i_N)\}\right) \simeq \operatorname{diag}\{\psi(u)\}.$$

Then for each $u \in [0,1]$ we have approximately the linear equation

$$\psi(u) = (\Gamma\otimes\Gamma)\operatorname{vec}(\Omega(u)) + \left((B+\Gamma)\otimes(B+\Gamma)\right)\psi(u) + (\Gamma\otimes\Gamma)\operatorname{diag}\{\psi(u)\}\operatorname{vec}(\Omega(u)).$$

We take vecs of the last term

$$\begin{aligned} \psi(u) &= (\Gamma\otimes\Gamma)\operatorname{vec}(\Omega(u)) + \left((B+\Gamma)\otimes(B+\Gamma)\right)\psi(u) + \left(\operatorname{vec}(\Omega(u)^\intercal)\otimes(\Gamma\otimes\Gamma)\right)\operatorname{vec}\left(\operatorname{diag}\{\psi(u)\}\right) \\ &= (\Gamma\otimes\Gamma)\operatorname{vec}(\Omega(u)) + \left((B+\Gamma)\otimes(B+\Gamma)\right)\psi(u) + \left(\operatorname{vec}(\Omega(u)^\intercal)\otimes(\Gamma\otimes\Gamma)\right)\Psi_N^\intercal\psi(u), \end{aligned}$$

where Ψ_N is the $N \times N^2$ matrix of zeros and ones defined in Magnus (1988, p109) that satisfies $\Psi_N^\intercal \text{diag}(D) = \text{vec}(D)$ for a diagonal matrix D. Therefore, it follows that

$$\psi(u) = \left(I_{N^2} - \left((B+\Gamma) \otimes (B+\Gamma) \right) - \left(\text{vec}(\Omega(u)^\intercal \otimes (\Gamma \otimes \Gamma) \right) \Psi_N^\intercal \right)^{-1} (\Gamma \otimes \Gamma) \, \text{vec}(\Omega(u)).$$

We also have

$$\begin{aligned} \text{vec}\left(E\left(\text{var}\left(\ell_t \,|\mathcal{F}_{t-1} \right) \right) \right) &= (G_t \otimes G_t) \, E \left(\Lambda_t \otimes \Lambda_t \right) \text{vec}\left(\Omega(t/T) \right) \\ &= \left(G(u) \otimes G(u) \right) \left(\text{vec}(\Omega(u)^\intercal \otimes I_{N^2} \right) \Psi_N^\intercal \psi(u). \end{aligned}$$

Furthermore,

$$\text{var}\left(E\left(\ell_t \,|\mathcal{F}_{t-1} \right) \right) = G_t \left(E\left(\lambda_t \lambda_t^\intercal \right) - i_N i_N^\intercal \right) G_t.$$

Together this gives an expression for the unconditional variance of ℓ_t, unfortunately, a very complicated one. Specifically,

$$\text{vec}\left(\text{var}\left(\ell_t \right) \right) = \left(G(u) \otimes G(u) \right) \left(\left(\text{vec}(\Omega(u)^\intercal \otimes I \right) \Psi_N^\intercal \psi(u) + \psi(u) \right).$$

This also gives an expression for the prediction error variance matrix.

In the scalar case

$$E\left(\lambda_t^2 - 1 \right) = \frac{\gamma^2 \omega(u)}{1 - (\beta+\gamma)^2 - \gamma^2 \omega(u)}.$$

$$\text{var}\left(\ell_t \right) = g(t/T)^2 \left(\frac{\gamma^2 \omega(u)}{1 - (\beta+\gamma)^2 - \gamma^2 \omega(u)} \left(1 + \omega(u) \right) + \omega(u) \right).$$

A.2 Profile GMM estimator

Let

$$G_t(\alpha, \beta) = \text{diag}\{ g_{1t}(\alpha_1, \beta_1), \ldots, g_{Nt}(\alpha_N, \beta_N) \}, \quad g_{1t}(\alpha_1, \beta_1) = \alpha_1 + \beta_1 (t/T - u).$$

Further define

$$\Lambda_t(\alpha, \beta; \theta) = \text{diag}\{ \lambda_{1t}(\alpha_1, \beta_1; \theta), \ldots, \lambda_{Nt}(\alpha_N, \beta_N; \theta) \}$$

$$\lambda_t(\alpha, \beta; \theta) = (I_N - B - \Gamma) \, i_N + B \lambda_{t-1}(\alpha, \beta; \theta) + G_t(\alpha, \beta)^{-1} \ell_{t-1}.$$

Then let

$$\rho_t(\alpha, \beta; \theta) = z_{t-1} \otimes \left(G_t(\alpha, \beta)^{-1} \Lambda_t(\alpha, \beta)^{-1} \ell_t - i_N \right)$$

$$M_T(\alpha,\beta;u,\theta)=\frac{1}{T}\sum_{t=1}^{T}K_h(t/T-u)\rho_t(\alpha,\beta;\theta).$$

The profiled local linear GMM estimator is defined as $\widehat{g}_\theta(u)=\widehat{\alpha}(u)$, where

$$(\widehat{\alpha}^\intercal(u),\widehat{\beta}^\intercal(u))^\intercal=\arg\min_{\alpha,\beta}\left\|M_T(\alpha,\beta;u,\theta)\right\|_S.$$

This would be very computationally demanding since it requires nonlinear optimization over $\mathbb{R}^{2N}$ for each value of $\theta\in\mathbb{R}^{2N^2}$ (in the general case) and each value of $u\in\{1/T,\dots(T-1)/T,1\}$. For this reason our two step approximation is more attractive, since each step is explicit.

We next show the connection of the profiled GMM estimator with our second round smoother. In the exactly identified case, with $z_{t-1}=1$ and dropping β, we see that α solves

$$\frac{1}{T}\sum_{t=1}^{T}K_h(t/T-u)\left(G_t(\alpha)^{-1}\Lambda_t(\alpha)^{-1}\ell_t-i_N\right)=0,$$

which is similar to

$$\frac{1}{T}\sum_{t=1}^{T}K_h(t/T-u)\left(G_t(\alpha)^{-1}\ell_t^\dagger-i_N\right)=0,$$

where $\ell_t^\dagger=\Lambda_t^{-1}\ell_t$, whose solution is similar to the solution of

$$\frac{1}{T}\sum_{t=1}^{T}K_h(t/T-u)\left(\ell_t^\dagger-\alpha\right)=0,$$

which is essentially our second round smoother applied to the prewhitened data.

A.3 Proof of Main Results

Proof of Theorem 1. The proof follows from the adaptation of Francisco-Fernández et al. (2003) employed by HLW1. We first give the explicit formula for the local linear estimator introduced in the text:

$$\begin{pmatrix}\widehat{\alpha}_{i,j}(u)\\ \widehat{\beta}_{i,j}(u)\end{pmatrix}=S_{T,i}(u)^{-1}\Delta_T^{-1}Q_{T,i,j}(u)$$

$$S_{T,i}(u)=\frac{1}{T}\sum_{t=1}^{T}D_{jt}K_h(t/T-u)\begin{pmatrix}1 & \frac{t/T-u}{h}\\ \frac{t/T-u}{h} & \left(\frac{t/T-u}{h}\right)^2\end{pmatrix}$$

$$Q_{T,i,j}(u) = \frac{1}{T}\sum_{t=1}^{T} D_{jt} K_h(t/T - u) \begin{pmatrix} 1 \\ \frac{t/T-u}{h} \end{pmatrix} \ell_{it},$$

where $\Delta_T = \text{diag}(1, h)$. We have

$$\frac{1}{T}\sum_{s=1}^{T} K_h((t-s)/T) D_{js} \to \tau_j = \lim_{T\to\infty} \frac{T_j}{T},$$

where T_j is the number of observations in category j. It follows that

$$\frac{\widehat{g}_{i,j}(t/T) - g_{i,j}(t/T)}{g_{i,j}(t/T)} = \frac{1}{T_j}\sum_{s=1}^{T} K_h((t-s)/T) D_{js} v_{is} + O_P(h^2),$$

$$\frac{\widetilde{g}_{i,j}(t/T) - g_{i,j}(t/T)}{g_{i,j}(t/T)} = \frac{1}{T_j}\sum_{s=1}^{T} K_h((t-s)/T) D_{js} (\zeta_{is} - 1) + O_P(h^2).$$

Proof of Theorem 2. This follows because

$$\begin{aligned}
\widehat{\Omega}(u) &= \frac{1}{T}\sum_{t=1}^{T} K_h(u - t/T) \left(\widehat{\zeta}_t - i_N\right) \left(\widehat{\zeta}_t - i_N\right)^{\intercal} \\
&= \frac{1}{T}\sum_{t=1}^{T} K_h(u - t/T) \left(\zeta_t - i_N\right) \left(\zeta_t - i_N\right)^{\intercal} \\
&+ \frac{1}{T}\sum_{t=1}^{T} K_h(u - t/T) \left(\widehat{\zeta}_t - \zeta_t\right) \left(\zeta_t - i_N\right)^{\intercal} \\
&+ \frac{1}{T}\sum_{t=1}^{T} K_h(u - t/T) \left(\zeta_t - i_N\right) \left(\widehat{\zeta}_t - \zeta_t\right)^{\intercal} \\
&+ \frac{1}{T}\sum_{t=1}^{T} K_h(u - t/T) \left(\widehat{\zeta}_t - \zeta_t\right) \left(\widehat{\zeta}_t - \zeta_t\right)^{\intercal}.
\end{aligned}$$

The second, third, and fourth terms are of smaller order in probability. This is equally true for the second round smoother.

Proof of Theorem 3. We establish condition 2.6 of Theorem 2 of Chen et al. (2003), i.e., the CLT for the term $\sqrt{T} M_T(\theta_0, \widehat{g})$, which is approximated by the linear term

$$\mathcal{L}_T(\theta_0, g_0) = M_T(\theta_0, g_0) + \Gamma_2(\theta_0, g_0) \circ (\widehat{g} - g_0), \tag{32}$$

where Γ_2 is the pathwise derivative of $M_T(\theta, g)$ with respect to the function g at the true parameter values. Here, the dependence of the moment function at time t is on all vectors

$g(1/T), \ldots, g((t-1)/T)$. We have

$$\begin{aligned}\sqrt{T}M_T(\theta_0, \widehat{g}) &= \frac{1}{\sqrt{T}}\sum_{t=1}^{T} z_{t-1} \otimes \left(\zeta_t(\theta_0, \widehat{g}) - i_N\right) \\ &= \frac{1}{\sqrt{T}}\sum_{t=1}^{T} z_{t-1} \otimes (\zeta_t - i_N) + \frac{1}{\sqrt{T}}\sum_{t=1}^{T} z_{t-1} \otimes \left(\zeta_t(\theta_0, \widehat{g}) - \zeta_t\right).\end{aligned}$$

First, we have

$$\begin{aligned}\zeta_t(\theta_0, \widehat{g}) - \zeta_t(\theta_0, g_0) &= \left(\Lambda_t(\theta_0, \widehat{g})^{-1}\widehat{G}_t^{-1} - \Lambda_t(\theta_0, g_0)^{-1}G_t^{-1}\right)\ell_t \\ &\simeq \Lambda_t(\theta_0, g_0)^{-1}\left(\widehat{G}_t^{-1} - G_t^{-1}\right)\ell_t + \left(\Lambda_t(\theta_0, \widehat{g})^{-1} - \Lambda_t(\theta_0, g_0)^{-1}\right)G_t^{-1}\ell_t \\ &\simeq -G_t^{-1}\left(\widehat{G}_t - G_t\right)\overbrace{\Lambda_t(\theta_0, g_0)^{-1}G_t^{-1}\ell_t}^{\zeta_t} \\ &\quad - \Lambda_t(\theta_0, g)^{-1}\left(\Lambda_t(\theta_0, \widehat{g}) - \Lambda_t(\theta_0, g_0)\right)\Lambda_t(\theta_0, g)^{-1}G_t^{-1}\ell_t,\end{aligned}$$

because diagonal matrices commute. Therefore, the correction term is

$$\begin{aligned}\tau_T &= \frac{1}{\sqrt{T}}\sum_{t=1}^{T} z_{t-1} \otimes \left(\zeta_t(\theta_0, \widehat{g}) - \zeta_t(\theta_0, g)\right) \\ &\simeq -\frac{1}{\sqrt{T}}\sum_{t=1}^{T} z_{t-1} \otimes \left(-G_t^{-1}\left(\widehat{G}_t - G_t\right)\zeta_t\right) - \frac{1}{\sqrt{T}}\sum_{t=1}^{T} z_{t-1} \otimes \left(\Lambda_t^{-1}\left(\Lambda_t(\theta_0, \widehat{g}) - \Lambda_t(\theta_0, g)\right)\zeta_t\right).\end{aligned}$$

We have for any g,

$$\begin{aligned}\lambda_t(\theta_0, g) &= (I_N - B - \Gamma)i_N + B\lambda_{t-1}(\theta_0, g) + \Gamma G_{t-1}^{-1}\ell_{t-1} \\ &= (I_N - B - \Gamma)i_N + B(I_N - B - \Gamma)i_N + B\Gamma G_{t-2}^{-1}\ell_{t-2} + \Gamma G_{t-1}^{-1}\ell_{t-1} + B^2\lambda_{t-2}(\theta_0, g) \\ &= \sum_{j=0}^{t} B^j(I_N - B - \Gamma)i_N + \sum_{j=0}^{t} B^j\Gamma G_{t-1-j}^{-1}\ell_{t-1-j} + \ldots.\end{aligned}$$

Therefore, for large enough t

$$\begin{aligned}\lambda_t(\theta_0, \widehat{g}) - \lambda_t(\theta_0, g_0) &= \sum_{j=0}^{t} B^j\Gamma\left(\widehat{G}_{t-1-j}^{-1} - G_{t-1-j}^{-1}\right)\ell_{t-1-j} \\ &\simeq -\sum_{j=0}^{\infty} B^j\Gamma G_{t-1-j}^{-1}\left(\widehat{G}_{t-1-j} - G_{t-1-j}\right)G_{t-1-j}^{-1}\ell_{t-1-j} \\ &\simeq -\sum_{j=0}^{\infty} B^j\Gamma G_{t-1}^{-1}\left(\widehat{G}_{t-1} - G_{t-1}\right)\ell_{t-1-j}^{*} \\ &= -\left(\sum_{j=0}^{\infty}\left(\ell_{t-1-j}^{*\intercal} \otimes B^j\Gamma\right)\right)\operatorname{vec}\left(G_{t-1}^{-1}\left(\widehat{G}_{t-1} - G_{t-1}\right)\right),\end{aligned}$$

because $\widehat{G}_{t-1-j} - G_{t-1-j} \simeq \widehat{G}_{t-1} - G_{t-1}$. We take vecs of a diagonal matrix. Let Ψ_N be the $N \times N^2$ matrix of zeros and ones defined in Magnus (1988, p109) that satisfies $\Psi_N^\intercal d = \text{vec}(D)$ for a diagonal matrix D with diagonal vector d. Therefore,

$$\begin{aligned}
\text{vec}\left(\Lambda_t(\theta_0, \widehat{g}) - \Lambda_t(\theta_0, g)\right) &= \Psi_N^\intercal \left(\lambda_t(\theta_0, \widehat{g}) - \lambda_t(\theta_0, g_0)\right) \\
&\simeq -\sum_{j=0}^{\infty} \Psi_N^\intercal B^j \Gamma G_{t-1}^{-1} \left(\widehat{G}_{t-1} - G_{t-1}\right) \ell_{t-1-j}^* \\
&\simeq -\sum_{j=0}^{\infty} \left(\ell_{t-1-j}^{*\intercal} \otimes \Psi_N^\intercal B^j \Gamma\right) \text{vec}\left(G_{t-1}^{-1} \left(\widehat{G}_{t-1} - G_{t-1}\right)\right).
\end{aligned}$$

Consider the term

$$\begin{aligned}
\tau_{T1} &= \frac{1}{\sqrt{T}} \sum_{t=1}^{T} z_{t-1} \otimes G_t^{-1} \left(\widehat{G}_t - G_t\right) \zeta_t \\
&= \frac{1}{\sqrt{T}} \sum_{t=1}^{T} z_{t-1} \otimes \left(\zeta_t^\intercal \otimes I_N\right) \text{vec}\left(G_t^{-1} \left(\widehat{G}_t - G_t\right)\right) \\
&\simeq \frac{1}{T\sqrt{T}} \sum_{t=1}^{T} z_{t-1} \otimes \left(\zeta_t^\intercal \otimes I_N\right) \sum_{j=1}^{J} \frac{1}{T_j} \sum_{s=1}^{T} K_h((s-t)/T) D_{js} \text{vec}\left(V_s\right) \\
&= \frac{1}{\sqrt{T}} \sum_{s=1}^{T} \sum_{j=1}^{J} \left(\frac{1}{T} \sum_{t=1}^{T} K_h((s-t)/T) z_{t-1} \otimes \left(\zeta_t^\intercal \otimes I_N\right)\right) D_{js} \text{vec}\left(V_s\right) \\
&\simeq \frac{1}{\sqrt{T}} \sum_{s=1}^{T} E\left(z_{s-1} i_N^\intercal \otimes I_N\right) \Psi_N^\intercal \sum_{j=1}^{J} D_{js} v_s \\
&= \frac{1}{\sqrt{T}} \sum_{s=1}^{T} \overline{F}_{1s} \left(\sum_{j=1}^{J} D_{js} v_s\right),
\end{aligned}$$

where $v_t = (v_{1t}, \ldots, v_{Nt})^\intercal$, where $v_{jt} = \lambda_{jt}\zeta_{jt} - 1$, while

$$\overline{F}_{1s} = E\left(z_{s-1} i_N^\intercal \otimes I_N\right) \Psi_N^\intercal.$$

Furthermore,

$$\begin{aligned}
\tau_{T2} &= \frac{1}{\sqrt{T}}\sum_{t=1}^{T} z_{t-1}\otimes\left(\Lambda_t^{-1}\left(\Lambda_t(\theta,\widehat{g})-\Lambda_t(\theta,g)\right)\zeta_t\right)\\
&= \frac{1}{\sqrt{T}}\sum_{t=1}^{T} z_{t-1}\otimes\left(\left(\zeta_t^{\intercal}\otimes\Lambda_t^{-1}\right)\mathrm{vec}\left(\Lambda_t(\theta,\widehat{g})-\Lambda_t(\theta,g)\right)\right)\\
&\simeq \frac{1}{\sqrt{T}}\sum_{t=1}^{T} z_{t-1}\otimes\left(\left(\zeta_t^{\intercal}\otimes\Lambda_t^{-1}\right)\sum_{j=0}^{\infty}\left(\ell_{t-1-j}^{*\intercal}\otimes\Psi_N^{\intercal}B^j\Gamma\right)\mathrm{vec}\left(G_{t-1}^{-1}\left(\widehat{G}_{t-1}-G_{t-1}\right)\right)\right)\\
&\simeq \frac{1}{\sqrt{T}}\sum_{t=1}^{T} z_{t-1}\otimes\left(\left(\zeta_t^{\intercal}\otimes\Lambda_t^{-1}\right)\sum_{j=0}^{\infty}\left(\ell_{t-1-j}^{*\intercal}\otimes\Psi_N^{\intercal}B^j\Gamma\right)\sum_{j=1}^{J}\frac{1}{T_j}\sum_{s=1}^{T}K_h((t-1-s)/T)D_{js}\mathrm{vec}\left(V_s\right)\right)\\
&\simeq \frac{1}{\sqrt{T}}\sum_{j=1}^{J}\sum_{s=1}^{T}\frac{1}{T_j}K_h((s-(t-1))/T)z_{t-1}\otimes\left(\left(\zeta_t^{\intercal}\otimes\Lambda_t^{-1}\right)\sum_{j=0}^{\infty}\left(\ell_{t-1-j}^{*\intercal}\otimes\Psi_N^{\intercal}B^j\Gamma\right)D_{js}\mathrm{vec}\left(V_s\right)\right)\\
&\simeq \frac{1}{\sqrt{T}}\sum_{j=1}^{J}\sum_{s=1}^{T}E\left(\left(z_{t-1}i_N^{\intercal}\otimes\Lambda_t^{-1}\right)\sum_{j=0}^{\infty}\left(\ell_{t-1-j}^{*\intercal}\otimes\Psi_N^{\intercal}B^j\Gamma\right)\right)\Psi_N^{\intercal}D_{js}v_s\\
&= \frac{1}{\sqrt{T}}\sum_{s=1}^{T}\overline{F}_{2s}\left(\sum_{j=1}^{J}D_{js}v_s\right),
\end{aligned}$$

where

$$\overline{F}_{2t}=\sum_{j=0}^{\infty}E\left(\left(z_{t-1}i_N^{\intercal}\otimes\Lambda_t^{-1}\right)\left(\ell_{t-1-j}^{*\intercal}\otimes\Psi_N^{\intercal}B^j\Gamma\right)\right)\Psi_N^{\intercal}.$$

In conclusion,

$$\sqrt{T}M_T(\theta_0,\widehat{g})\simeq\frac{1}{\sqrt{T}}\sum_{t=1}^{T}\left(z_{t-1}\otimes(\zeta_t-i_N)+\overline{F}_t v_t\right)\equiv\frac{1}{\sqrt{T}}\sum_{t=1}^{T}\psi_t(\theta_0,g_0).$$

The same arguments apply to $\sqrt{T}M_T(\theta_0,\widetilde{g})$ except that we replace v_t in the above expansion by ζ_t-i_N.

We have

$$\begin{aligned}
\widehat{G}_t-G_t &= \mathrm{diag}\left(\prod_{j=1}^{J}\left(\widehat{g}_{1,j}(t/T)^{D_{jt}}-g_{1,j}(t/T)^{D_{jt}}\right),\ldots,\prod_{j=1}^{J}\left(\widehat{g}_{N,j}(t/T)^{D_{jt}}-g_{N,j}(t/T)^{D_{jt}}\right)\right)\\
&= \mathrm{diag}\left(\sum_{j=1}^{J}D_{jt}\left(\widehat{g}_{1,j}(t/T)-g_{1,j}(t/T)\right),\ldots,\sum_{j=1}^{J}D_{jt}\left(\widehat{g}_{N,j}(t/T)-g_{N,j}(t/T)\right)\right),
\end{aligned}$$

and therefore,

$$G_t^{-1}(\widehat{G}_t - G_t) = \sum_{j=1}^{J} \operatorname{diag}\left(\frac{1}{T_j}\sum_{s=1}^{T} K_h((t-s)/T)D_{js}v_{1s}, \ldots, \frac{1}{T_j}\sum_{s=1}^{T} K_h((t-s)/T)D_{js}v_{Ns}\right) + O_P(h^2)$$
$$= \sum_{j=1}^{J} \frac{1}{T_j}\sum_{s=1}^{T} K_h((t-s)/T)D_{js}V_s + O_P(h^2),$$

where $V_s = \operatorname{diag}(v_{1s}, \ldots, v_{Ns})$.

B Additional tables and figures

B.1 Long-run illiquidty trends

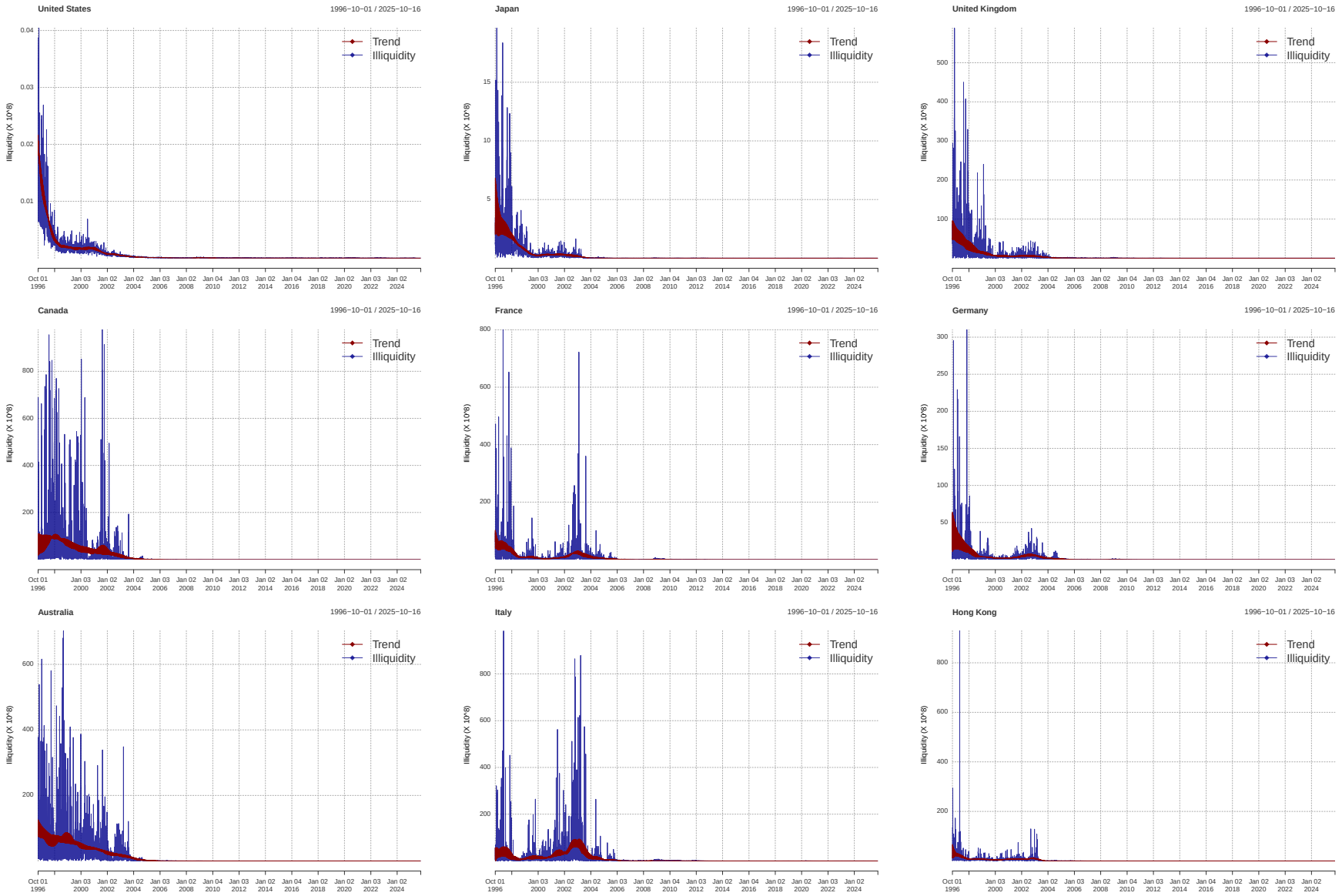

Figure 7: Illiquidity series and its trend estimates.

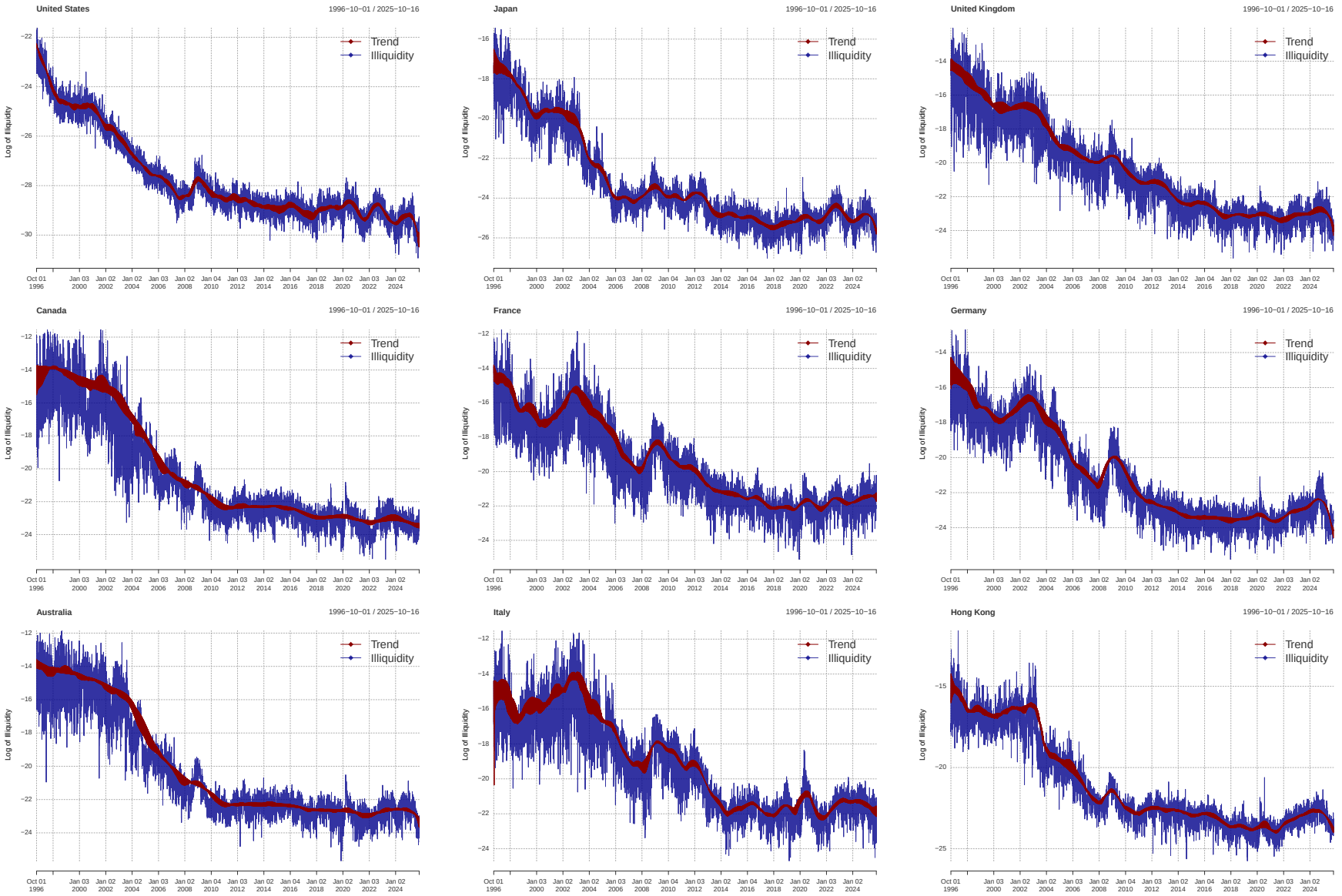

Figure 8: Log of illiquidity series and its trend estimates.

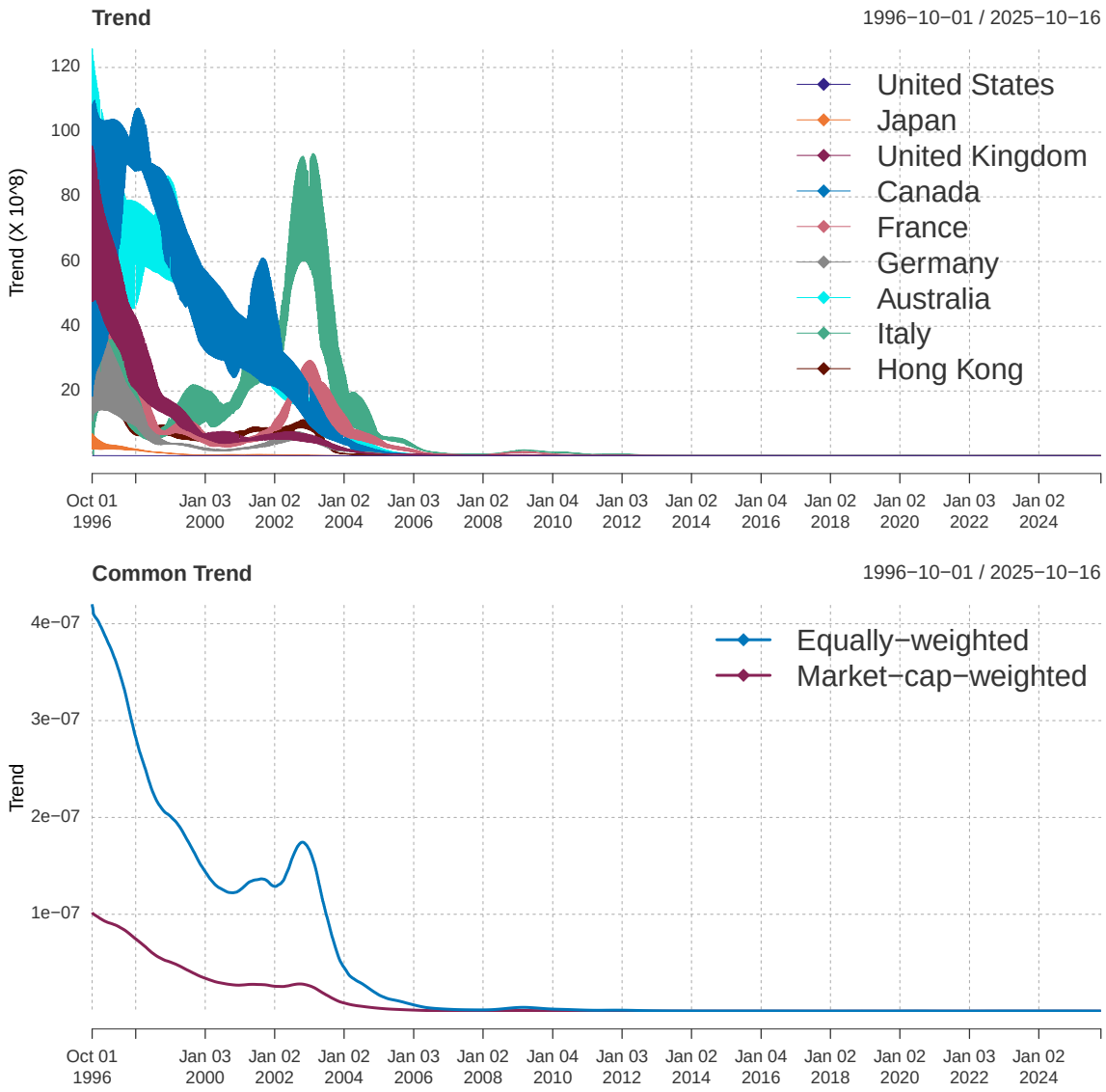

Figure 9: Illiquidity trends and the common trend.

B.2 Short-run illiquidity dynamics

We start with the special case where $B = D_B$ is a diagonal matrix, which can be estimated using single equation methods. We focus on two scenarios. First, we consider GARPD model with the parameter matrix decomposition $\Gamma = D_\Gamma + D^* W^\top$ where W contains both equally-weighted and market-cap-weighted schemes. This specification yields four parameters to characterize the dynamics for each country.[6] Second, we estimate the Γ

[6]We also consider the cases where W contains equal weights or market-cap based weights separately. Results reported in Table 4 suggest that considering a single weighting scheme might be too restrictive to

matrix directly, which is more flexible but requires estimating $N + 1$ parameters for every country. The estimates for all models are reported in Table 4.

Table 4: Estimates of the λ_t process parameters in the special case of $B = D_B$ using single equation method.

	$D_{B,ii}$	$D_{\Gamma,ii}$	D^*_{i1}	D^*_{i2}	B									Γ									ω
W equal weighting																							
United States	0.729	0.134	0.030		0.729									0.137	0.003	0.003	0.003	0.003	0.003	0.003	0.003	0.003	0.107
Japan	0.764	0.151	0.048			0.764								0.005	0.157	0.005	0.005	0.005	0.005	0.005	0.005	0.005	0.036
United Kingdom	0.653	0.157	0.075				0.653							0.008	0.008	0.165	0.008	0.008	0.008	0.008	0.008	0.008	0.116
Canada	0.744	0.159	0.106					0.744						0.012	0.012	0.012	0.170	0.012	0.012	0.012	0.012	0.012	-0.008
France	0.626	0.132	0.141						0.626					0.016	0.016	0.016	0.016	0.148	0.016	0.016	0.016	0.016	0.101
Germany	0.774	0.128	0.076							0.774				0.008	0.008	0.008	0.008	0.008	0.136	0.008	0.008	0.008	0.022
Australia	0.824	0.117	0.063								0.824			0.007	0.007	0.007	0.007	0.007	0.007	0.124	0.007	0.007	-0.004
Italy	0.636	0.133	0.158									0.636		0.018	0.018	0.018	0.018	0.018	0.018	0.018	0.150	0.018	0.074
Hong Kong	0.709	0.163	0.088										0.709	0.010	0.010	0.010	0.010	0.010	0.010	0.010	0.010	0.173	0.040
W market cap weighting																							
United States	0.725	0.031	0.128		0.725									0.129	0.009	0.005	0.005	0.004	0.003	0.003	0.001	0.001	0.116
Japan	0.756	0.141	0.105			0.756								0.081	0.148	0.004	0.004	0.003	0.003	0.002	0.001	0.001	-0.002
United Kingdom	0.716	0.138	0.122				0.716							0.094	0.008	0.143	0.004	0.003	0.003	0.002	0.001	0.001	0.023
Canada	0.770	0.149	0.109					0.770						0.084	0.007	0.005	0.153	0.003	0.003	0.002	0.001	0.001	-0.029
France	0.728	0.122	0.151						0.728					0.116	0.010	0.006	0.006	0.127	0.004	0.003	0.001	0.001	-0.001
Germany	0.776	0.133	0.093							0.776				0.071	0.006	0.004	0.003	0.003	0.135	0.002	0.001	0.001	-0.001
Australia	0.810	0.130	0.078								0.810			0.060	0.005	0.003	0.003	0.002	0.002	0.131	0.001	0.000	-0.017
Italy	0.713	0.126	0.181									0.713		0.139	0.012	0.008	0.007	0.005	0.005	0.004	0.127	0.001	-0.020
Hong Kong	0.740	0.146	0.134										0.740	0.103	0.009	0.006	0.005	0.004	0.003	0.003	0.001	0.146	-0.020
Combine																							
United States	0.725	0.036	0.002	0.121	0.725									0.130	0.008	0.005	0.005	0.004	0.003	0.003	0.001	0.001	0.116
Japan	0.764	0.152	0.052	-0.010		0.764								-0.002	0.157	0.005	0.005	0.005	0.005	0.006	0.006	0.006	0.044
United Kingdom	0.646	0.155	0.106	-0.073			0.646							-0.044	0.007	0.163	0.009	0.010	0.010	0.010	0.011	0.011	0.166
Canada	0.744	0.156	0.103	0.026				0.744						0.032	0.013	0.013	0.169	0.012	0.012	0.012	0.012	0.012	-0.029
France	0.623	0.126	0.176	-0.079					0.623					-0.041	0.014	0.016	0.017	0.144	0.018	0.018	0.019	0.019	0.154
Germany	0.767	0.127	0.096	-0.053						0.767				-0.030	0.007	0.009	0.009	0.009	0.137	0.010	0.010	0.010	0.062
Australia	0.823	0.118	0.069	-0.025							0.823			-0.011	0.006	0.007	0.007	0.007	0.007	0.125	0.007	0.008	0.015
Italy	0.625	0.124	0.202	-0.098								0.625		-0.053	0.016	0.018	0.019	0.020	0.020	0.020	0.145	0.022	0.147
Hong Kong	0.708	0.163	0.090	-0.004									0.708	0.007	0.010	0.010	0.010	0.010	0.010	0.010	0.010	0.173	0.043
Estimate Γ																							
United States					0.720									0.129	0.005	0.011	0.007	-0.002	0.001	0.001	0.002	0.007	0.120
Japan						0.686								-0.027	0.178	-0.013	0.016	0.008	0.009	0.009	0.001	0.020	0.113
United Kingdom							0.654							-0.060	0.013	0.163	0.004	0.006	0.012	0.018	0.005	0.017	0.168
Canada								0.708						0.053	0.004	0.009	0.182	0.025	-0.002	0.023	0.012	0.018	-0.033
France									0.623					-0.028	0.019	0.006	0.017	0.137	0.035	0.016	0.026	-0.001	0.149
Germany										0.763				-0.017	-0.001	0.011	0.009	0.002	0.140	0.010	0.015	0.012	0.056
Australia											0.810			-0.026	0.002	0.001	0.011	0.003	0.016	0.131	0.006	0.008	0.038
Italy												0.623		-0.061	0.016	0.038	0.028	0.007	0.006	0.026	0.147	0.005	0.164
Hong Kong													0.666	-0.046	0.024	-0.005	0.024	0.007	0.016	0.010	0.009	0.176	0.119

Note: Under the restriction that the B matrix is diagonal, we carry out the estimation line by line.

We further consider two groups of models. In the first group, we estimate the parameter matrices B and Γ directly, with three specifications: both matrices unrestricted, B diagonal with unrestricted Γ, and Γ diagonal with unrestricted B. In the second group, we consider the GAP model structure where the parameter matrices are decomposed as $B = D_B + B^* W^\top$, $\Gamma = D_\Gamma + D^* W^\top$. Here, W denotes the weighting scheme, taken as equal-weighting, market-cap weighting, or a combination of the two. The estimates for the two

fully capture the dynamics.

groups of models are reported in Table 5 and Table 6 respectively.

Table 5: Estimates of the λ_t process parameters in the GAP specification ($B = D_B + B^* W^\top, \Gamma = D_\Gamma + D^* W^\top$).

	β_{ii}	b_{i1}	b_{i2}	γ_{ii}	δ_{i1}	δ_{i2}	B									Γ									ω
												W equal weighting													
United States	0.683	0.024		0.130	0.020		0.685	0.003	0.003	0.003	0.003	0.003	0.003	0.003	0.003	0.133	0.002	0.002	0.002	0.002	0.002	0.002	0.002	0.002	0.143
Japan	0.634	0.071		0.211	0.016		0.008	0.642	0.008	0.008	0.008	0.008	0.008	0.008	0.008	0.002	0.212	0.002	0.002	0.002	0.002	0.002	0.002	0.002	0.069
United Kingdom	0.481	0.232		0.206	-0.027		0.026	0.026	0.507	0.026	0.026	0.026	0.026	0.026	0.026	-0.003	-0.003	0.203	-0.003	-0.003	-0.003	-0.003	-0.003	-0.003	0.108
Canada	0.696	0.047		0.185	0.082		0.005	0.005	0.005	0.701	0.005	0.005	0.005	0.005	0.005	0.009	0.009	0.009	0.194	0.009	0.009	0.009	0.009	0.009	-0.011
France	0.508	0.216		0.171	0.054		0.024	0.024	0.024	0.024	0.532	0.024	0.024	0.024	0.024	0.006	0.006	0.006	0.006	0.177	0.006	0.006	0.006	0.006	0.050
Germany	0.714	0.074		0.146	0.053		0.008	0.008	0.008	0.008	0.008	0.722	0.008	0.008	0.008	0.006	0.006	0.006	0.006	0.006	0.151	0.006	0.006	0.006	0.014
Australia	0.550	0.293		0.234	-0.010		0.033	0.033	0.033	0.033	0.033	0.033	0.583	0.033	0.033	-0.001	-0.001	-0.001	-0.001	-0.001	-0.001	0.233	-0.001	-0.001	-0.067
Italy	0.503	0.227		0.173	0.077		0.025	0.025	0.025	0.025	0.025	0.025	0.025	0.529	0.025	0.009	0.009	0.009	0.009	0.009	0.009	0.009	0.182	0.009	0.019
Hong Kong	0.590	0.098		0.219	0.037		0.011	0.011	0.011	0.011	0.011	0.011	0.011	0.011	0.601	0.004	0.004	0.004	0.004	0.004	0.004	0.004	0.004	0.223	0.057
												W market cap weighting													
United States	0.791	0.088		-0.079	0.107		0.858	0.006	0.004	0.003	0.002	0.002	0.002	0.001	0.001	0.003	0.007	0.004	0.004	0.003	0.003	0.002	0.001	0.001	0.094
Japan	0.555	0.304		0.216	-0.030		0.233	0.576	0.013	0.011	0.009	0.008	0.006	0.003	0.002	-0.023	0.214	-0.001	-0.001	-0.001	-0.001	-0.001	-0.000	-0.000	-0.046
United Kingdom	0.509	0.457		0.191	-0.063		0.351	0.030	0.528	0.017	0.013	0.011	0.009	0.004	0.003	-0.048	-0.004	0.189	-0.002	-0.002	-0.002	-0.001	-0.001	-0.000	-0.094
Canada	0.620	0.481		0.194	0.023		0.369	0.032	0.020	0.638	0.014	0.012	0.010	0.004	0.003	0.018	0.002	0.001	0.195	0.001	0.001	0.000	0.000	0.000	-0.318
France	0.498	0.608		0.170	0.030		0.467	0.041	0.025	0.022	0.515	0.015	0.012	0.005	0.004	0.023	0.002	0.001	0.001	0.171	0.001	0.001	0.000	0.000	-0.306
Germany	0.627	0.394		0.166	0.013		0.302	0.026	0.016	0.014	0.011	0.636	0.008	0.003	0.002	0.010	0.001	0.001	0.000	0.000	0.166	0.000	0.000	0.000	-0.199
Australia	0.569	0.566		0.223	-0.046		0.434	0.038	0.023	0.021	0.016	0.014	0.581	0.005	0.003	-0.035	-0.003	-0.002	-0.002	-0.001	-0.001	0.222	-0.000	-0.000	-0.312
Italy	0.504	0.626		0.172	0.055		0.481	0.042	0.026	0.023	0.018	0.016	0.013	0.509	0.004	0.042	0.004	0.002	0.002	0.002	0.001	0.001	0.172	0.000	-0.357
Hong Kong	0.558	0.348		0.227	0.006		0.267	0.023	0.014	0.013	0.010	0.009	0.007	0.003	0.560	0.005	0.000	0.000	0.000	0.000	0.000	0.000	0.000	0.227	-0.139
												Combine													
United States	0.989	-0.046	-0.163	0.014	0.067	0.056	0.859	-0.016	-0.012	-0.011	-0.010	-0.009	-0.008	-0.006	-0.006	0.064	0.011	0.010	0.010	0.009	0.009	0.009	0.008	0.008	0.083
Japan	0.657	0.141	-0.211	0.200	0.015	0.023	-0.146	0.659	0.007	0.008	0.010	0.010	0.011	0.014	0.014	0.019	0.203	0.003	0.003	0.002	0.002	0.002	0.002	0.002	0.175
United Kingdom	0.499	0.255	-0.114	0.197	0.003	-0.040	-0.059	0.021	0.522	0.024	0.025	0.025	0.026	0.027	0.028	-0.030	-0.002	0.195	-0.001	-0.001	-0.001	-0.000	0.000	0.000	0.200
Canada	0.679	0.259	-0.497	0.176	0.069	0.080	-0.353	-0.004	0.008	0.689	0.015	0.016	0.019	0.025	0.026	0.069	0.013	0.011	0.187	0.010	0.010	0.009	0.008	0.008	0.234
France	0.517	-0.081	0.595	0.155	0.150	-0.106	0.447	0.031	0.016	0.013	0.524	0.006	0.003	-0.004	-0.005	-0.065	0.010	0.012	0.013	0.169	0.014	0.015	0.016	0.016	-0.230
Germany	0.681	0.168	-0.186	0.149	0.061	-0.019	-0.124	0.006	0.011	0.012	0.013	0.695	0.015	0.017	0.018	-0.008	0.006	0.006	0.006	0.006	0.156	0.006	0.007	0.007	0.145
Australia	0.559	0.511	-0.510	0.216	-0.043	0.087	-0.334	0.023	0.036	0.038	0.042	0.044	0.605	0.052	0.054	0.062	0.001	-0.001	-0.002	-0.002	-0.003	0.213	-0.004	-0.004	0.180
Italy	0.502	0.265	-0.143	0.154	0.146	-0.124	-0.081	0.020	0.024	0.024	0.025	0.026	0.027	0.530	0.029	-0.079	0.008	0.011	0.012	0.013	0.013	0.014	0.170	0.016	0.200
Hong Kong	0.591	0.202	-0.238	0.207	0.035	0.007	-0.160	0.007	0.013	0.014	0.016	0.017	0.018	0.020	0.612	0.009	0.004	0.004	0.004	0.004	0.004	0.004	0.004	0.211	0.196

Table 6: Estimates of the λ_t process parameters using GMM (B, Γ).

	B									Γ									ω
Diagonal B Γ																			
United States	0.800									0.152									0.048
Japan		0.769									0.161								0.069
United Kingdom			0.788									0.133							0.079
Canada				0.772									0.163						0.065
France					0.790									0.127					0.083
Germany						0.811									0.131				0.058
Australia							0.792									0.158			0.051
Italy								0.779									0.128		0.093
Hong Kong									0.783									0.152	0.065
Diag B																			
United States	0.746									0.122	0.006	0.011	0.005	-0.000	0.000	-0.001	0.002	0.005	0.104
Japan		0.652								-0.031	0.201	-0.006	0.012	0.010	0.002	0.009	0.002	0.019	0.129
United Kingdom			0.650							-0.064	0.010	0.166	0.003	-0.001	0.008	0.027	0.010	0.018	0.174
Canada				0.690						0.051	0.021	0.008	0.195	0.013	0.006	0.022	0.010	0.031	-0.046
France					0.647					-0.036	0.019	0.011	0.024	0.145	0.020	0.018	0.022	-0.011	0.140
Germany						0.743				-0.038	0.000	0.011	0.015	0.004	0.146	0.008	0.012	0.016	0.083
Australia							0.681			-0.066	0.001	-0.001	0.028	-0.003	0.015	0.203	0.011	0.010	0.121
Italy								0.632		-0.092	0.017	0.033	0.036	0.006	0.012	0.016	0.154	0.016	0.171
Hong Kong									0.643	-0.051	0.025	-0.002	0.016	0.004	0.011	0.010	0.012	0.201	0.131
Diagonal Γ																			
United States	0.484	0.026	0.044	0.019	-0.014	0.014	-0.012	0.005	0.020	0.204									0.210
Japan	0.036	0.634	-0.044	0.020	0.031	0.014	0.010	0.016	0.054		0.190								0.041
United Kingdom	-0.051	0.044	0.566	-0.041	0.018	0.036	0.061	0.038	0.022			0.183							0.122
Canada	-0.113	0.020	0.010	0.617	0.092	-0.006	0.076	0.003	0.015				0.201						0.086
France	0.028	0.088	0.032	0.038	0.420	0.126	-0.007	0.088	-0.032					0.172					0.046
Germany	-0.003	-0.018	0.043	0.008	0.037	0.627	0.029	0.061	0.035						0.166				0.016
Australia	-0.020	0.034	0.010	0.025	-0.017	0.066	0.692	0.061	0.014							0.161			-0.025
Italy	-0.169	0.010	0.137	0.072	0.015	0.046	0.045	0.454	0.028								0.167		0.194
Hong Kong	-0.089	0.074	-0.012	0.052	0.021	0.052	0.026	0.010	0.543									0.200	0.123
Full B Γ																			
United States	0.849	-0.017	-0.009	-0.009	-0.004	0.024	-0.016	0.016	-0.020	0.097	0.013	0.010	0.008	0.000	-0.006	0.006	-0.000	0.011	0.047
Japan	0.249	0.590	-0.039	-0.034	-0.024	0.005	0.022	0.036	0.019	-0.068	0.218	-0.002	0.019	0.015	0.000	0.003	-0.004	0.015	-0.021
United Kingdom	0.252	0.046	0.501	-0.040	0.030	0.035	0.030	0.069	-0.063	-0.077	-0.003	0.196	0.005	-0.012	-0.003	0.017	-0.002	0.034	-0.017
Canada	0.293	-0.013	-0.020	0.676	-0.058	0.029	0.030	0.050	-0.155	-0.110	0.028	0.005	0.193	0.025	-0.002	0.022	0.002	0.076	-0.071
France	0.182	0.070	0.015	0.013	0.511	0.056	-0.019	0.061	-0.061	-0.038	0.000	0.001	0.017	0.171	0.009	0.021	0.013	0.002	-0.023
Germany	0.044	-0.061	0.021	-0.040	0.007	0.692	0.099	0.023	-0.022	-0.036	0.023	0.005	0.024	0.005	0.154	-0.027	0.007	0.027	0.054
Australia	-0.247	0.053	0.087	0.018	-0.018	0.123	0.584	0.035	-0.048	0.001	-0.002	-0.021	0.023	-0.001	-0.017	0.227	0.002	0.019	0.184
Italy	0.126	0.004	-0.034	0.068	-0.061	0.118	-0.070	0.563	0.068	-0.089	0.012	0.041	0.010	0.016	-0.015	0.034	0.167	-0.012	0.054
Hong Kong	-0.186	0.013	0.000	0.012	0.041	-0.006	0.035	-0.005	0.612	0.008	0.025	0.002	0.010	-0.004	0.011	-0.005	0.012	0.211	0.214

B.3 Variance decomposition and connectedness

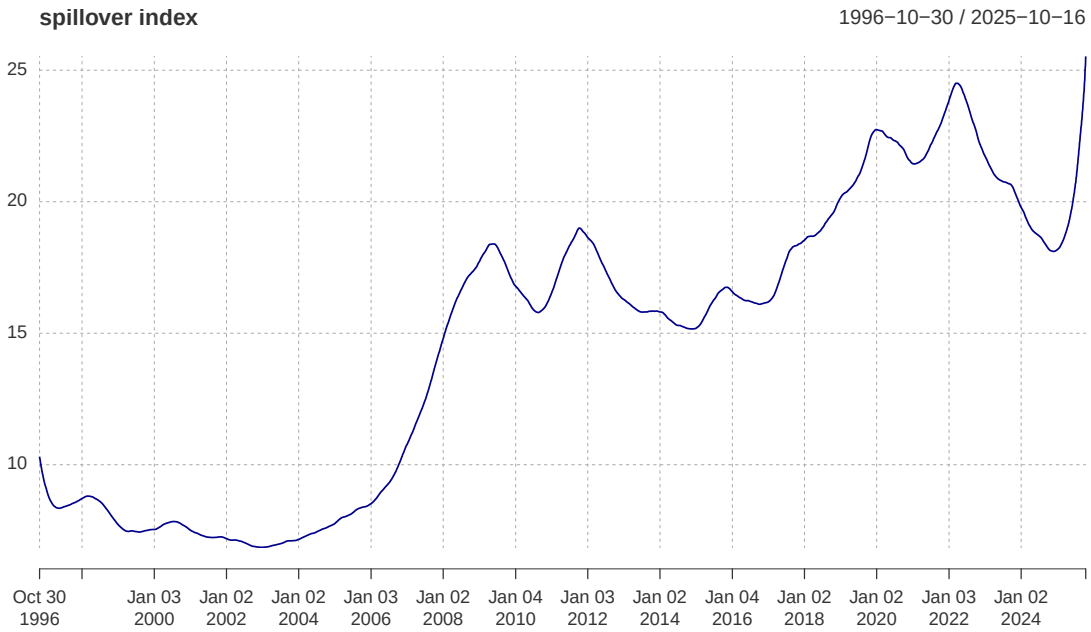

Figure 10: Spillover Index for horizon $h = 22$ (Cholesky decomposition).

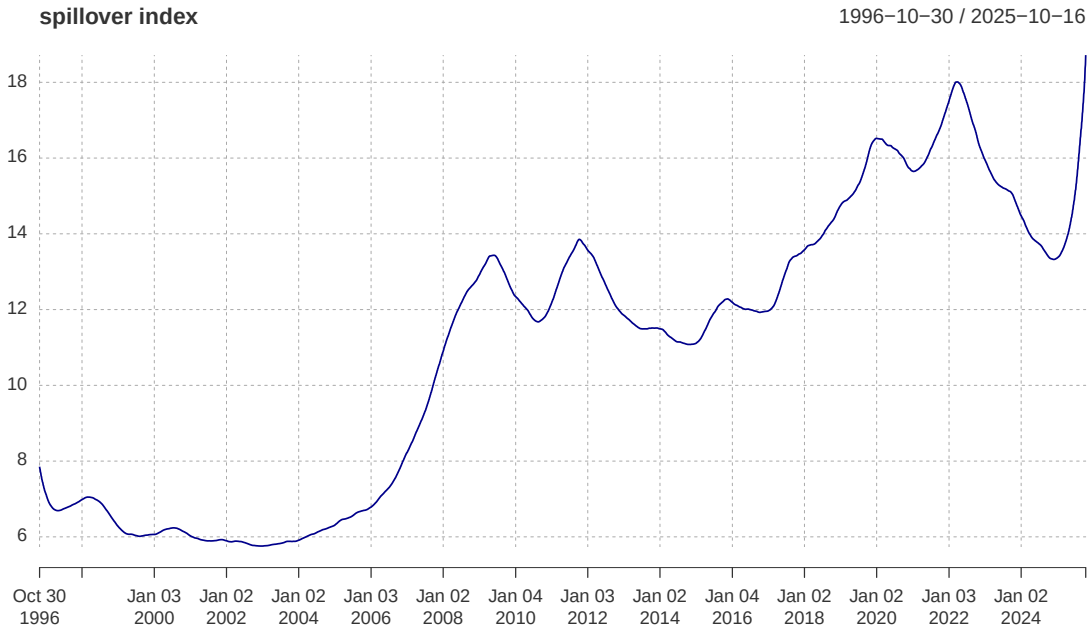

Figure 11: Spillover Index for horizon $h = 22$ (Spectral decomposition).